An ice–climate oscillatory framework for Dansgaard–Oeschger cycles

Laurie C. Menviel[1] ✉, *Luke C. Skinner*[2], *Lev Tarasov*[3] *and Polychronis C. Tzedakis*[4]

Abstract | Intermediate glacial states were characterized by large temperature changes in Greenland and the North Atlantic, referred to as Dansgaard–Oeschger (D–O) variability, with some transitions occurring over a few decades. D–O variability included changes in the strength of the Atlantic meridional overturning circulation (AMOC), temperature changes of opposite sign and asynchronous timing in each hemisphere, shifts in the mean position of the Intertropical Convergence Zone and variations in atmospheric CO_2. Palaeorecords and numerical studies indicate that the AMOC, with a tight coupling to Nordic Seas sea ice, is central to D–O variability, yet, a complete theory remains elusive. In this Review, we synthesize the climatic expression and processes proposed to explain D–O cyclicity. What emerges is an oscillatory framework of the AMOC–sea-ice system, arising through feedbacks involving the atmosphere, cryosphere and the Earth's biogeochemical system. Palaeoclimate observations indicate that the AMOC might be more sensitive to perturbations than climate models currently suggest. Tighter constraints on AMOC stability are, thus, needed to project AMOC changes over the coming century as a response to anthropogenic carbon emissions. Progress can be achieved by additional observational constraints and numerical simulations performed with coupled climate–ice-sheet models.

The Atlantic meridional overturning circulation (AMOC) (BOX 1) is a central part of the Earth's climate and biogeochemical system, as it transports heat, dissolved salts, nutrients and carbon throughout the ocean's basins. The AMOC is dependent on North Atlantic Deep Water (NADW) formation, which, at present, primarily occurs in the Nordic Seas, with a minor component in the Labrador Sea[1]. Despite recent weakening[2], the AMOC has mostly been in a strong state over at least the past 2,000 years, and probably most of the Holocene[3–5]. To a first order, a stable and strong AMOC can be explained by the Stommel salt-advection feedback[6], whereby a strong AMOC is associated with a strong North Atlantic current and, thus, advection of salty tropical Atlantic waters to the North Atlantic, enhancing deep-water formation at high latitudes. Owing to anthropogenic greenhouse gas emissions, it is likely that the AMOC will weaken over the coming century[7], with implications for the climate, ecosystems and continental ice sheets. However, there remain significant uncertainties associated with future rates of AMOC changes and the potential of reaching a tipping point, particularly as the AMOC in current coupled climate models has been deemed too stable[8,9]. It is, thus, crucial to better understand the processes that affect the AMOC, as well as the subsequent response of the climate and carbon cycle.

Progress can be achieved by studying past millennial-scale climatic variability (FIG. 1), such as Dansgaard–Oeschger (D–O) cyclicity, during which the AMOC is inferred to have varied substantially[10] (FIG. 1a). First highlighted in Greenland ice cores spanning the last glacial period and deglaciation (~115–11.6 thousand years ago (ka)), D–O cycles are characterized by a decadal-scale air-temperature increase of 5–16 °C in Greenland (a D–O warming event), leading to an interstadial peak (warm conditions)[11–14] (FIG. 1b). After this interstadial peak, Greenland temperatures gradually decrease over a few centuries to a millennium and then abruptly drop to stadial (cold conditions).

Marine sediment cores from the North Atlantic have revealed that some of the D–O stadials identified in Greenland ice cores are associated with thick layers of ice-rafted debris (IRD), inferred to be sourced from fast-flowing terrestrial ice[15–17]. The majority of these thick IRD layers have a high detrital carbonate content, indicating Hudson Strait provenance[18] and, thus implying discharges from the Laurentide Ice Sheet (LIS) and IRD transport by icebergs. These high-IRD episodes are known as Heinrich events and occur within longer cold phases, referred to as Heinrich stadials[19,20]. Twenty-five D–O stadials and interstadials have been identified within the last glacial–interglacial cycle, 15 of which occurred during the relatively mild glacial conditions of

[1]*Climate Change Research Centre, PANGEA, University of New South Wales, Sydney, NSW, Australia.*

[2]*Department of Earth Sciences, University of Cambridge, Cambridge, UK.*

[3]*Department of Physics and Physical Oceanography, Memorial University of Newfoundland, St John's, NL, Canada.*

[4]*Environmental Change Research Centre, Department of Geography, University College London, London, UK.*

✉*e-mail: l.menviel@unsw.edu.au*

https://doi.org/10.1038/s43017-020-00106-y

Key points

- Abrupt warming events in Greenland and the North Atlantic, referred to as Dansgaard–Oeschger (D–O) events, were associated with a strengthening of the Atlantic meridional overturning circulation (AMOC), and changes in the global climate and carbon cycle.
- AMOC changes, with a tight coupling to Nordic Seas sea ice, strongly affect the climate and marine carbon cycle, and, in turn, the ice-sheet mass balance. Resultant changes in oceanic wind stress, ocean heat content and salinity feed back on the AMOC.
- Owing to the different timescales of the feedbacks, self-sustained AMOC oscillations could emerge during intermediate glacial states. The boundary conditions of intermediate glacial states (size of ice sheets, Bering Strait throughflow and atmospheric CO_2 concentration) appear to be key in enabling these oscillations.
- Perturbations other than changes in meltwater input, including changes in atmospheric CO_2 or Northern Hemisphere ice-sheet height and extent, can lead to, and may be required for, D–O variability.
- The relatively large and frequent AMOC changes associated with D–O variability suggest a relatively low AMOC stability during intermediate glacial states. This low stability is not evident in all numerical experiments performed with coupled climate models, implying that some might either overestimate the AMOC stability or have a mismatch in the required background state for the low-AMOC-stability regime.
- Additional observations on the location and strength of North Atlantic Deep Water formation and its link with sea ice, as well as its improved representation in climate models, are needed to better constrain future climate projections.

Marine Isotope Stage 3 (MIS 3; 59.4–24 ka)[13,14]. By contrast, Heinrich stadials were less frequent, with only six events identified during the last glacial interval and subsequent deglaciation[18,21] (FIG. 1).

D–O cycles and Heinrich events are not restricted to the last glacial period: ice-core and speleothem records suggest prevalent D–O variability over at least the past 800 kyr (REF.[22]), and sediment cores from the North Atlantic document IRD layers accompanied by a drop in sea-surface temperature (SST) during glacial periods and deglaciations of the Pleistocene[21–33]. As evidenced by benthic oxygen isotopic ratio ($\delta^{18}O$) records, which, to a first order, provide an estimate of the volume of continental ice sheets[34], maximum D–O climate variability appears to occur in an intermediate glacial state, when the Northern Hemisphere continental ice sheets are of intermediate size. This intermediate state corresponds to a North Atlantic $\delta^{18}O$ range of 3.5–4.2‰, a globally averaged benthic $\delta^{18}O$ stack in the range 4–4.7‰ and a relative sea level ~45–80 m lower than present[25,33,35–37]. Although strict background thresholds for the occurrence of D–O variability are difficult to define precisely, it is clear that D–O variability has generally been suppressed during peak interglacial and peak glacial states[25].

Palaeoproxy records and numerical simulations provide strong evidence that D–O variability (including Heinrich stadials unless specified otherwise) was associated with changes in the strength of the AMOC[10,38–40]. These AMOC variations, accompanied by shifts in the seasonal sea-ice extent in the Nordic Seas, Labrador Sea and, potentially, northern North Atlantic[41,42], induced changes in global climate and biogeochemistry[43–46]. However, the sequence of events and mechanisms that led to D–O climate variability is still highly debated. Each stadial is associated with a higher IRD abundance in the North Atlantic, indicative of enhanced iceberg discharges[20,25,47–51]. To test the climatic effects of iceberg discharges into the North Atlantic, a freshwater flux is artificially added into the North Atlantic in coupled climate models (termed freshwater hosing experiments)[52]. As the addition of freshwater into the North Atlantic reduces the surface-water density, it weakens deep-water formation and the AMOC, leading to colder conditions over the North Atlantic and Greenland[52,53]. It was, therefore, initially suggested that D–O climatic variability is due to the AMOC response to variations in meltwater input into the North Atlantic[38,47]. However, this hypothesis would mean that the amplitudes of stadials (that is, the difference between Heinrich and non-Heinrich stadials) are entirely determined by the magnitude of the forcing. In addition, it has also been suggested that iceberg discharges follow, instead of precede, North Atlantic cooling[20]. As an alternative to the freshwater hosing proposition, internal oscillations of the ocean–sea-ice system have been suggested[54]. However, these oscillations have been simulated in only a few climate models forced under specific boundary conditions[55–58]. Abrupt AMOC changes have also been simulated as a response to gradual changes in LIS height[59] and atmospheric CO_2 concentration[60]. However, the processes leading to these changes in ice sheets, meltwater or CO_2 also need to be constrained and integrated into a D–O framework. To date, no Earth system model has fully replicated all observed climatic and biogeochemical characteristics associated with D–O variability, especially under relevant boundary conditions. D–O variability, including prognostic changes in continental ice sheets and CO_2, remains to be simulated by Earth system models.

In this Review, we assess the global climatic changes associated with D–O stadials, Heinrich stadials and interstadials, and the evidence for their link with AMOC changes. We then discuss the possible mechanisms put forward to explain D–O variability and propose a self-sustained oscillatory framework involving all components of the Earth system. Finally, we conclude by considering the implications of the oscillatory framework for AMOC stability.

D–O climatic variability and AMOC changes

In this section, we examine the climatic changes associated with D–O variability, as deduced from palaeoproxy records from Greenland and the North Atlantic region, where this climatic variability was first highlighted. We also review the millennial-scale climatic variability that occurs concurrently in distal regions and their link to D–O variability, as revealed by palaeoclimate modelling (FIG. 2). We show that both proximal and distal climatic variability can be explained by variations in AMOC strength in combination with dynamical responses at high southern latitudes and in the North Pacific.

D–O stadials. Greenland ice-core records suggest that the transitions into interstadials are followed by a slow cooling trend, lasting 500 to more than 2,000 years, which ends with a decadal-scale cooling back to stadial conditions[61] (FIG. 1b), with a total temperature change of 6.5–16.5 °C (REF.[14]). This cooling is also recorded in the

Box 1 | **The Atlantic meridional overturning circulation**

The figure shows the annual mean sea-surface temperature (SST) in the North Atlantic[231], as well as the fast-flowing surface western boundary currents in the Atlantic — the Gulf Stream and its northeast extension, the North Atlantic Current — which bring warm and salty water to the North Atlantic. Subsequent advection of this water to the Nordic Seas, coupled with heat loss to the atmosphere and sea-ice formation, induces intermediate-depth convection and the formation of North Atlantic Deep Water (NADW)[232]. NADW, one of today's main deep-water masses, primarily forms in the Nordic Seas, with a minor component in the Labrador Sea[1], and flows southward at a depth of ~1,500–3,500 m in the Atlantic along the deep western boundary current, below Antarctic Intermediate Water and above Antarctic Bottom Water (AABW). These water masses, along with recirculated deep water from the Indian and Pacific Oceans, mix in the Southern Ocean to form Circumpolar Deep Water, which then flows at depth into the Indian and Pacific Oceans.

The zonal integral of the surface and deep currents in the Atlantic defines the Atlantic meridional overturning circulation (AMOC). Estimating the AMOC transport is a challenge as it requires making measurements across the Atlantic. The RAPID Meridional Overturning Circulation and Heatflux Array, established in 2004, has measured an AMOC transport at 26.5°N of ~18.7 ± 5.6 Sv (where 1 Sv = 10^6 m^3 s^{-1}), with large seasonal and interannual variability[233]. The more recent Overturning in the Subpolar North Atlantic Program (OSNAP) observing system, which measures the AMOC over two sections southwest and east of Greenland (between 53°N and 59.5°N), reported a mean AMOC transport of 16.8 Sv for the period 2014–2016 (REF.[1]). The AMOC has a crucial role in heat, freshwater and nutrient transport. The oceanic poleward heat transport at 26.5°N in the North Atlantic has been estimated at ~1.3 PW. The AMOC contributes 60–88% of this oceanic heat transport[78,234], with the remainder being due to the wind-driven gyre circulation. The AMOC strength depends on the density of surface waters in the NADW formation region, with the density being a function of salinity and temperature. Dynamical effects, such as the strength of the subpolar gyre (SPG), which itself is modulated by North Atlantic wind stress, also affect NADW formation[216,218].

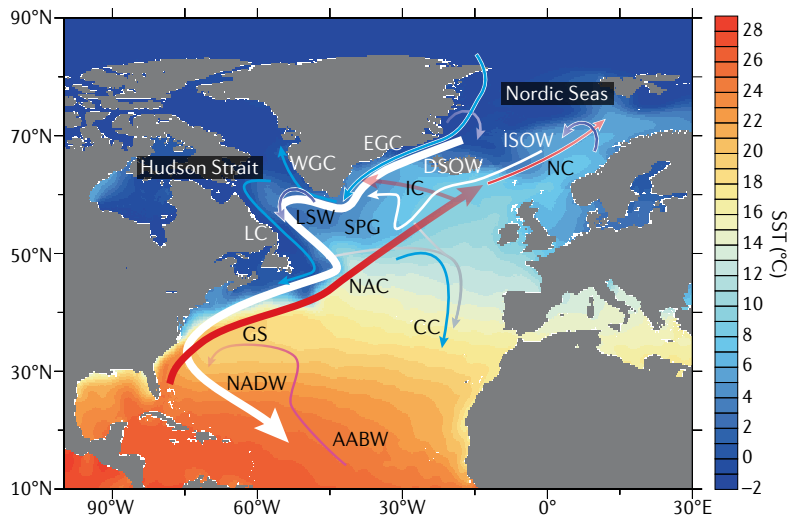

Surface and subsurface currents

Warm
GS = Gulf Stream
NAC = North Atlantic Current
NC = Norwegian Current
IC = Irminger Current

Cold
EGC = East Greenland Current
WGC = West Greenland Current
LC = Labrador Current
CC = Canary Current

Deep current
LSW = Labrador Sea Water
DSOW = Denmark Strait Overflow Water
ISOW = Iceland–Scotland Overflow Water

Abyssal current

Deep-water formation

Norwegian Sea, with the spring sea-ice cover advancing to ~62°N (REFS[41,42]), and in the northern North Atlantic, with an equatorward shift of the polar front to ~57°N (REFS[17,20,49,50]). Notable cooling is also recorded over southern Europe[62–64], as well as in marine sediment cores from the western Iberian margin and the Mediterranean Sea, with an estimated ~1.5 °C decrease in SST during D–O stadials[26,65,66] (FIG. 1d).

Planktonic $\delta^{18}O$ records reveal the presence of a strong halocline in the Nordic Seas and the northeastern North Atlantic during stadials[48,67]. It is proposed that these North Atlantic coolings and freshenings, associated with the presence of IRD layers, are linked to AMOC weakening during interstadial to stadial transitions[47]. Furthermore, proxy records indicative of changes in oceanic circulation, such as North Atlantic records of the sedimentary $^{231}Pa/^{230}Th$ (REFS[10,68,69]) (FIG. 1a), benthic foraminifera carbon isotope ratio ($\delta^{13}C$)[51,70–73], neodymium isotope ratios (εNd)[68,74,75] and the concentration of carbonate ions ($[CO_3^{2-}]$) in South Atlantic bottom water[76], support recurrent AMOC weakening during each stadial of MIS 3.

Although the atmospheric poleward heat transport accounts for 78% of the total heat transport at 35°N (REF.[77]), the oceanic meridional heat transport in the North Atlantic, with the AMOC being its main contributor[78] (BOX 1), accounts for the total oceanic heat transport north of 30°N. AMOC weakening thus leads to considerable cooling in the North Atlantic and sea-ice advance over the Labrador and Nordic Seas[53,79] (FIG. 2a). Greater sea-ice cover in the Nordic Seas increases surface albedo and reduces heat loss from the ocean to the atmosphere, thus leading to substantial cooling over Greenland[80]. Palaeoproxy records suggest that increased sea-ice cover, reduced air–sea heat exchange and weaker deep-ocean convection could also induce subsurface ocean warming (≥1 °C) in the Nordic Seas[41,42,67,81–83]. Annual mean subsurface warming in the Nordic Seas resulting from AMOC weakening, such as that inferred for D–O stadials, is not necessarily simulated in freshwater hosing experiments because of the dominant effect of reduced advection of warm North Atlantic waters into the Nordic Seas and the occurrence of deep-ocean convection[84] (FIG. 3a). However, as deep-ocean convection occurs in winter close to the sea-ice edge, summer sea-ice melting and increased stratification could lead to subsurface warming in summer, as inferred from proxy records.

As the AMOC leads to northward oceanic meridional heat transport at all latitudes in the Atlantic Basin[85], a weaker AMOC induces warming in the South Atlantic, extending from the surface to intermediate depths, due to weaker 'heat piracy' (REFS[86–88]) (FIG. 2a). Proxy records indeed suggest slightly warmer conditions during D–O stadials than interstadials at mid and high southern latitudes, with a potential southward shift of the thermal subtropical and sub-Antarctic fronts in the South Atlantic[89–91] and an ~1 °C SST increase in the sub-Antarctic and South Pacific[92–94] (FIG. 2a). High-resolution Antarctic ice-core records, synchronized with Greenland ice cores through atmospheric methane (CH_4) evolution, also suggest that all stadials of the last glacial period were associated with a multi-millennial ~1 °C warming in Antarctica[44,95–97] (FIG. 1g). This north–south asynchrony, termed the thermal bipolar see-saw[88,98], was initially described by a thermodynamic model in which AMOC changes

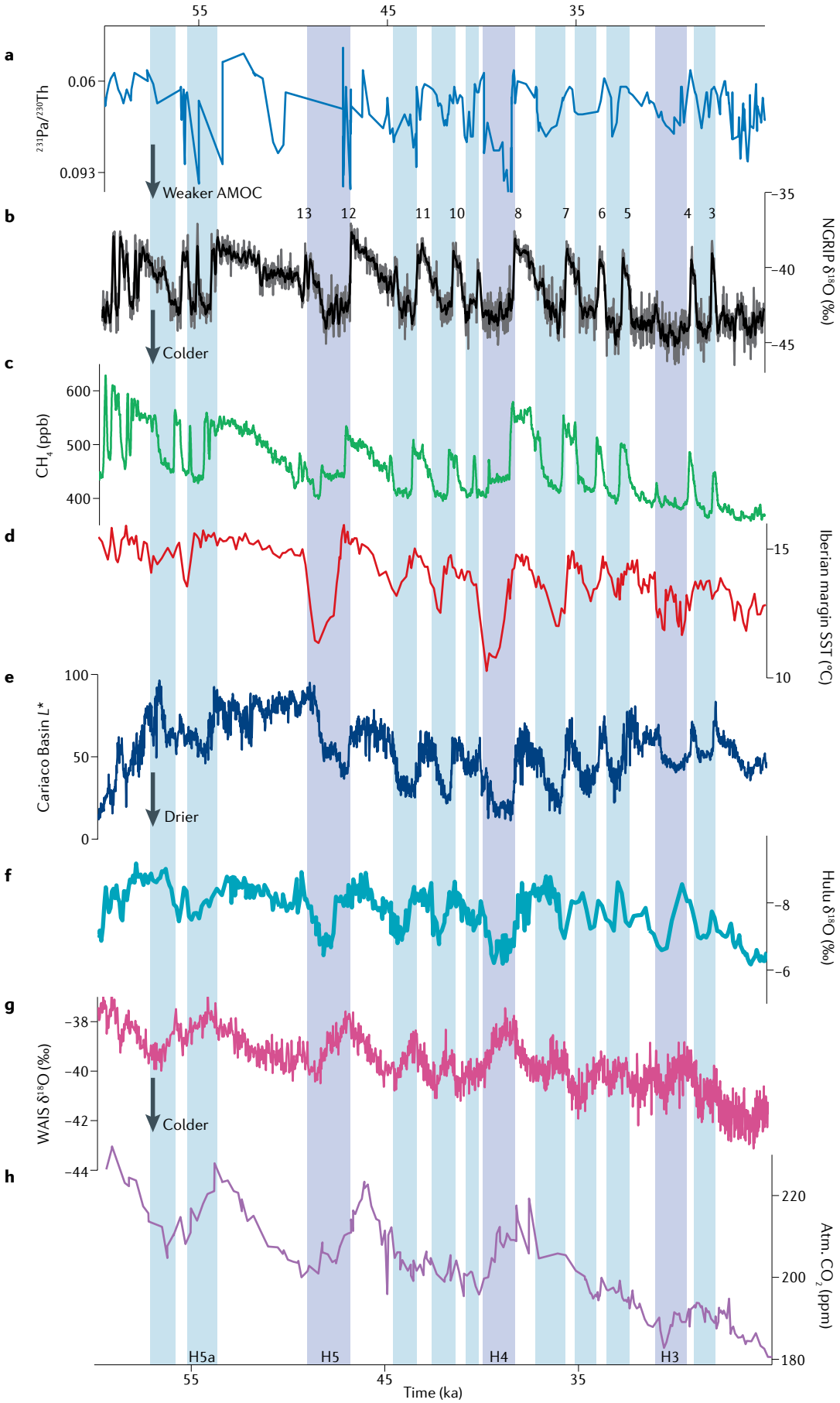
a
b
c
d
e
f
g
h
55
45
35
$^{231}Pa/^{230}Th$
0.06
0.093
Weaker AMOC
13
12
11
10
8
7
6
5
4
3
NGRIP $\delta^{18}O$ (‰)
−35
−40
−45
Colder
CH_4 (ppb)
600
500
400
Iberian margin SST (°C)
15
10
Cariaco Basin L^*
100
50
0
Drier
Hulu $\delta^{18}O$ (‰)
−8
−6
WAIS $\delta^{18}O$ (‰)
−38
−40
−42
−44
Colder
Atm. CO_2 (ppm)
220
200
180
H5a
H5
H4
H3
Time (ka)

Fig. 1 | **Proxy records showing D–O variability across Marine Isotope Stage 3.** **a** | $^{231}Pa/^{230}Th$ from the Bermuda Rise[10]. **b** | North Greenland Ice Core Project (NGRIP) oxygen isotope ratio ($\delta^{18}O$) on the Greenland Ice Core Chronology 2005 (GICC05)[229], with the interstadials numbered. **c** | Atmospheric methane (CH_4) concentration from the West Antarctic Ice Sheet (WAIS) Divide ice core[159]. **d** | Sea-surface temperature (SST) estimate based on the alkenone unsaturation index ($U^{k'}_{37}$) from sediment core MD01-2443 retrieved from the Iberian margin[26]. **e** | Total reflectance (L^*) of sediment from the Cariaco Basin[45]. **f** | $\delta^{18}O$ record from Hulu Cave, China[43]. **g** | WAIS $\delta^{18}O$ record[97]. **h** | Atmospheric CO_2 concentration from Siple[46] and Talos[230] Domes. Blue shading indicates Dansgaard–Oeschger (D–O) stadials and purple shading indicates Heinrich (H) stadials 5 through to 3. These proxy records show that each stadial is associated with weakening of the Atlantic meridional overturning circulation (AMOC) (panel **a**), cooling over Greenland (panel **b**) and the North Atlantic (panel **d**), low atmospheric CH_4 content (panel **c**), dry conditions in the northern tropics (panel **e**) and a weaker East Asian monsoon (panel **f**), indicating a southward shift of the Intertropical Convergence Zone. D–O stadials are associated with a small $\delta^{18}O$ increase over Antarctica (panel **g**). Heinrich stadials are associated with an increase in CO_2 (panel **h**) and a more pronounced $\delta^{18}O$ increase over Antarctica, indicating much warmer conditions. Data for panel **a** from REF.[10]. Data for panel **b** from REF.[229]. Data for panel **c** from REF.[159]. Data for panel **d** from REF.[26]. Data for panel **e** from REF.[45]. Data for panel **f** from REF.[43]. Data for panel **g** from REF.[97]. Data for panel **h** from REFS[46,230].

modulate the meridional ocean heat transport[88], increasing the Southern Ocean heat content, decreasing Southern Ocean sea-ice cover and leading to warming over Antarctica, owing to ocean heat release.

Climate-modelling experiments in which the AMOC is artificially weakened and proxy records (including pollen records, speleothems and the geochemical composition of marine and lake sediment) provide evidence for changes in the hydrological cycle during D–O stadials. Lower SSTs in the North Atlantic, coupled to a strengthening of the subtropical high-pressure system in the North Atlantic, lead to drier conditions over southern Europe and the Mediterranean region[53,64,79,99–102] (FIG. 2c). For example, numerical simulations performed with climate models under glacial conditions estimate a reduction in precipitation of approximately 10 cm yr^{-1} over southern Europe[79]. Stadials were also associated with drier conditions in the northern tropical Atlantic (~−10 cm yr^{-1})[45,79] (FIG. 1e) and wetter conditions in the southern tropical Atlantic (~+10 cm yr^{-1})[69,79], with a stronger South American monsoon[103–105] (FIG. 2c). Furthermore, analyses of marine sediment cores and freshwater hosing experiments suggest a weaker Indian summer monsoon during stadials[45,53,79,106–109]. Although higher $\delta^{18}O$ values recorded in speleothems from China (FIG. 1f) have been interpreted as reflecting a weaker East Asian monsoon during stadials[43,110,111], this is not consistently supported by numerical simulations performed with coupled climate models[79,107] (FIG. 2c). The latitudinal location of maximum precipitation, the Intertropical Convergence Zone (ITCZ), lies at the energy flux equator, the position of which depends on the tropospheric air-temperature difference between the hemispheres[112]. Cooler conditions over, at least part of, the high northern latitudes and warmer conditions at high southern latitudes thus induce a southward shift of the ITCZ in the Atlantic Ocean and Indian Ocean sectors during stadials[39,53,79,107,108,112], consistent with the hydrological changes observed in the palaeorecords.

D–O stadials are, therefore, characterized by the following climatic changes, consistent with a change in oceanic meridional heat transport in the Atlantic: sea-ice advance in the Nordic Seas; cooling over Greenland (~−12 °C), the North Atlantic (~−1.5 °C at mid latitudes and ~−4 °C close to the sea-ice front) and Europe; and small-amplitude (~1 °C) warming at mid and high southern latitudes. D–O stadials are also associated with drier conditions in southern Europe and over the northern tropics, while the southern tropics become wetter, consistent with a southward shift of the ITCZ. Numerical simulations suggest that the observed climatic and oceanic geochemical changes are consistent with a weaker AMOC.

Heinrich stadials. In Greenland ice cores, the amplitude of the $\delta^{18}O$ and correlated temperature changes that occur during D–O and Heinrich stadials are similar (FIG. 1b), even though Heinrich stadials are usually longer than non-Heinrich stadials[14,28,44]. Proxy records suggest that sea-ice cover is perennial in the Norwegian Sea and reaches 62°N (REFS[41,42]) during Heinrich stadials, and that the cooling in the northern North Atlantic is similar to that during D–O stadials[20,49,50]. However, additional data are needed to better constrain the full extent of the sea-ice advance in the Nordic Seas and northern North Atlantic during Heinrich stadials. Over southern Europe, the cooling is usually larger during Heinrich stadials than D–O stadials[62–64]. In marine sediment cores from the western Iberian margin and the Mediterranean Sea, the SST anomalies are twice as large (~−3 °C) for Heinrich stadials[26,65,66] (FIGS 1d,2a, 2b).

Heinrich events are characterized by a particularly high IRD abundance in North Atlantic sediments[20,25,48–51], indicating sustained iceberg discharge and transport to core sites. In addition, compared with D–O stadials, Heinrich stadials are associated with higher-amplitude climatic anomalies in the North Atlantic and far-field regions (as detailed below), thus pointing to a very weak or even fully shutdown AMOC[15,38,54,113]. Numerical simulations performed with coupled climate models indeed suggest that an AMOC shutdown reduces the meridional oceanic heat transport to the North Atlantic by ~40% (~−0.8 PW at 30°N)[53,79,114] (FIG. 2b), thus leading to strong North Atlantic cooling (~3–6 °C). As deep-ocean convection brings surface waters that are close to freezing point to depth, reduced deep-water formation in the Nordic Seas leads to subsurface warming[84] (FIG. 3). In addition, as deep-water formation in the Nordic Seas weakens, so does transport through the East Greenland Current, which brings cold water to the northwestern Atlantic. As a result, the subsurface temperature increases in the Greenland Sea, the Labrador Sea and in the northwestern Atlantic[84,115,116]. The geographical location and depth of the subsurface warming is dependent on changes in the site of deep-water formation and associated changes in subsurface currents.

Proxies for oceanic circulation provide further support for a very weak AMOC during Heinrich stadials. For example, the sedimentary $^{231}Pa/^{230}Th$ in the North Atlantic increases towards the production ratio[10,68,117] (FIG. 1a), indicating a notable reduction in the southward advection of Pa at depth in the North Atlantic, in agreement with an AMOC shutdown. Furthermore, $\delta^{13}C$ decreases in the intermediate and deep North

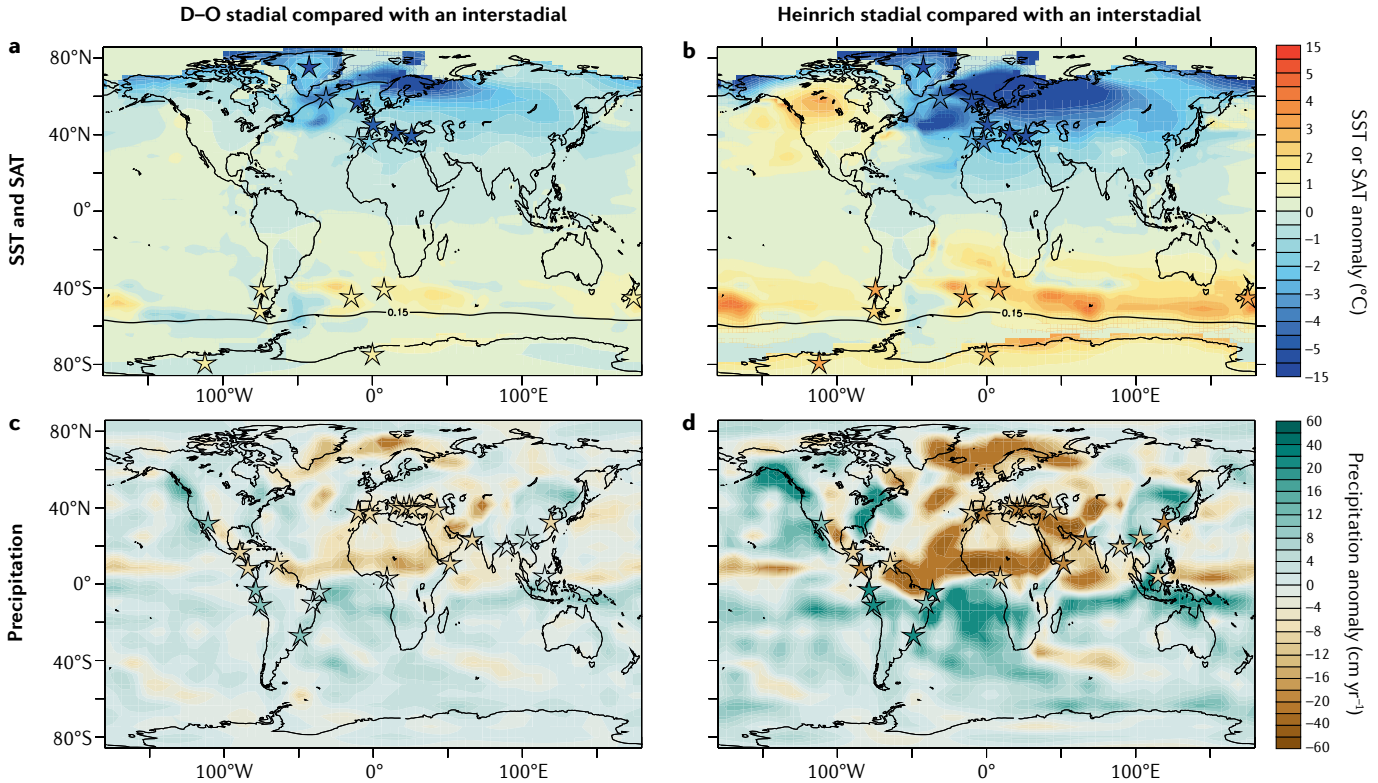

Fig. 2 | **Climatic anomalies associated with D–O and Heinrich stadials compared with an interstadial peak.** Stadials are associated with colder and drier conditions in the North Atlantic and Europe, drier conditions in the northern tropics, wetter conditions in the southern tropics and warmer conditions in the South Atlantic. The amplitude of these changes is larger during Heinrich stadials, with notable warming over the Southern Ocean and Antarctica. **a**,**b** | Annual mean sea-surface temperature (SST) and surface-air temperature (SAT) anomalies for a Dansgaard–Oeschger (D–O) stadial (~37.1 ka; panel **a**) and a Heinrich stadial (~39.1 ka; panel **b**) relative to an interstadial peak (~38.1 ka), as simulated in LOVECLIM[39]. The black line represents the 15% concentration sea-ice contour. **c**,**d** | Precipitation anomalies for the D–O stadial (panel **c**) and Heinrich stadial (panel **d**) relative to the interstadial peak, as simulated in LOVECLIM[39]. Stars indicate quantitative (SST) and qualitative (SAT and precipitation) estimates (see Supplementary Tables S1 and S2) of the climatic changes associated with D–O variability of Marine Isotope Stage 3 discussed in the main text.

Atlantic[71,72,118–120] (although the signal is muted for Heinrich stadials 2 and 3)[40,73], and $[CO_3^{2-}]$ decreases in the deep South Atlantic, both indicating reduced NADW transport[76].

Hydrological changes are also generally larger during Heinrich than D–O stadials. Relative to an interstadial, conditions are much drier over southern Europe, the Mediterranean (~−20 cm yr^{-1})[64,99–102] and the northern tropical Atlantic (~−20 to −40 cm yr^{-1})[45,121,122]. The Indian summer monsoon is weaker (~−20 to −40 cm yr^{-1})[45,106,108,109,123], and possibly also the East Asian monsoon[43,110,111] (FIGS 1e,1f,2d). By contrast, wetter conditions prevail in the southern tropical Atlantic (~+10–30 cm yr^{-1})[69], and the South American monsoon is stronger[103–105]. Heinrich stadials have, thus, been associated with more spatially extensive and more extreme southward shifts of the ITCZ[39,45,53,112,124–126] (FIG. 2d).

The greater amplitude of the AMOC changes, and the associated changes in oceanic meridional heat transport, during Heinrich stadials leads to more pronounced warming at mid to high southern latitudes (FIG. 2b). Proxy records suggest a southward shift of the thermal subtropical and sub-Antarctic fronts in the South Atlantic[89–91], a 2–3 °C (±0.5 °C) SST increase in the sub-Antarctic and South Pacific[92–94], and a multi-millennial 2–3 °C (±1 °C) increase in surface air temperature over Antarctica[44,95,97] (FIG. 1g).

Freshwater hosing experiments performed with climate models consistently simulate a South Atlantic SST increase, of up to 3 °C, as a result of an AMOC cessation[53,79] (FIG. 2b). However, not all simulations display a SST increase in the South Pacific Ocean, and the magnitude of the simulated temperature increase over Antarctica is lower (~0.5 °C) than suggested by proxy records[53,79,127,128]. The magnitudes of the surface temperature increase over Antarctica and the Southern Ocean are, however, correlated, confirming the important role of ocean processes in Antarctic warming[79], even if regional differences in the temperature response over Antarctica are most likely due to atmospheric processes[127]. These simulations thus highlight the limits of the bipolar see-saw theory: an AMOC weakening and associated change in meridional oceanic heat transport might not explain the full magnitude of the high-southern-latitude warming. Instead of just passively responding to AMOC changes, changes in Southern Ocean dynamics might need to be invoked[98,129]. Enhanced deep-ocean convection in the Southern

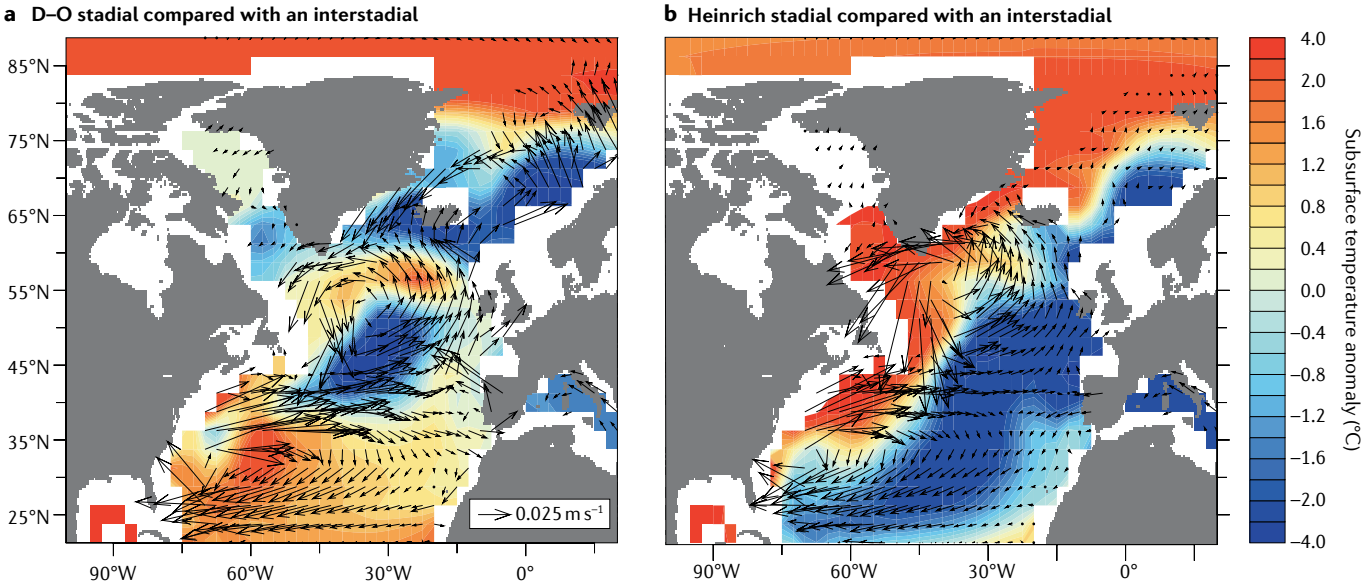

Fig. 3 | **Subsurface temperature anomalies associated with D–O and Heinrich stadials compared with an interstadial peak.** Annual subsurface (346–694-m depth) temperature anomalies for a Dansgaard–Oeschger (D–O) stadial (~37.1 ka; panel **a**) and a Heinrich stadial (~39.1 ka; panel **b**) relative to an interstadial peak (~38.1 ka), as simulated in LOVECLIM[39]. The subsurface currents ($m\,s^{-1}$), indicated by black arrows, are overlaid.

Ocean during stadials[130,131], resulting from stronger and/or poleward-shifted Southern Hemisphere westerlies or reduced surface buoyancy, would increase the ocean meridional heat transport towards Antarctica[132]. In turn, this change would lead to surface ocean warming, sea-ice decrease and warmer conditions at high southern latitudes[132–135].

Even if the response of Southern Hemisphere westerlies to Heinrich stadials is poorly constrained, temperature changes in the North Atlantic could affect the Southern Hemisphere westerlies through an atmospheric tropical bridge[127,128]. As the ITCZ corresponds to the ascending branch of the Hadley cell, a southward ITCZ shift strengthens the Northern Hemisphere Hadley cell, owing to increased heat transport by the Northern Hemisphere Hadley cell to compensate for reduced northward oceanic heat transport[136]. This strengthening of the Northern Hemisphere Hadley cell in turn weakens the Southern Hemisphere Hadley cell. An associated weakening of the Southern Hemisphere subtropical jet would shift the Southern Hemisphere eddy-driven jet poleward and strengthen the Southern Hemisphere surface westerlies[137,138]. Although additional constraints on the response of Southern Hemisphere westerlies to North Atlantic cooling are needed, Antarctic ice-core isotopic records[139] indicate a strengthening and poleward shift of the Southern Hemisphere westerlies during stadials. This rapid atmospheric teleconnection between the North Atlantic and the Southern Ocean would be superposed onto a slower oceanic teleconnection.

Enhanced deep-ocean convection in the Southern Ocean during Heinrich stadials, potentially resulting from strengthening of the Southern Hemisphere surface westerlies, could explain the observed concurrent increase in CO_2 concentration (FIG. 1h), through increased upwelling of carbon-rich deep waters to the surface[46,132,134,140,141]. Deep-ocean convection in the Southern Ocean would lead to further sea-ice retreat[132], which could also contribute to the CO_2 rise[142]. Increased dissolved oxygen content and reduced ventilation ages in the deep South Atlantic during Antarctic warm events may corroborate this possibility by pointing to increased Southern Ocean ventilation[91,130,131].

Palaeoproxy records suggest that the formation of North Pacific Intermediate Water (NPIW) was probably stronger during Heinrich stadial 1 than during either the Last Glacial Maximum (LGM; ~20 ka) or the Holocene[143–145]. Numerical simulations show that, when the Bering Strait is closed, an AMOC shutdown could enhance NPIW formation[143,146–148] through a reduction in moisture transport from the Atlantic to the Pacific, coupled to reduced precipitation in the western equatorial Pacific, owing to the southward shift of the ITCZ. Increased surface salinity in the northwest Pacific could then strengthen NPIW formation, which would be reinforced through the Stommel feedback by enhanced advection of low-latitude saline waters. The associated increase in heat transport to the northeast Pacific could lead to warmer and wetter conditions over North America (FIG. 2b), thus, potentially affecting the LIS mass balance. In addition, through enhanced ventilation of carbon-rich intermediate North Pacific waters, a stronger NPIW would contribute to a CO_2 increase[149].

The climatic imprint of Heinrich stadials is, thus, similar to that of D–O stadials, but Heinrich stadials are longer, and the amplitude of their climatic and oceanic geochemical changes is generally larger, consistent with a weaker AMOC (FIG. 4). A weaker AMOC is also consistent with larger changes in Northern Hemisphere ice sheets and iceberg discharges into the North Atlantic during Heinrich stadials. The larger high-southern-latitude warming and considerable CO_2 increase occurring

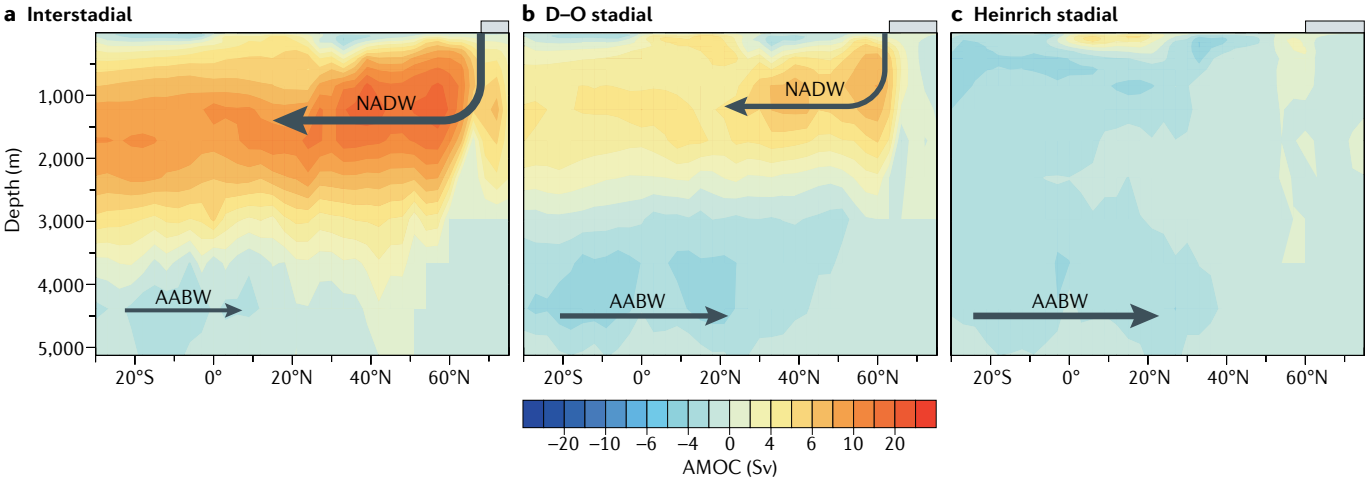

Fig. 4 | **Possible AMOC states for stadials and interstadials.** Possible states of the Atlantic meridional overturning circulation (AMOC) for interstadials (panel **a**), Dansgaard–Oeschger (D–O) stadials (panel **b**) and Heinrich stadials (panel **c**). Positive values indicate a clockwise ocean circulation associated with North Atlantic Deep Water (NADW), whereas negative values indicate an anticlockwise circulation associated with Antarctic Bottom Water (AABW). The grey areas at the surface represent possible winter sea-ice extension in the Nordic Seas.

during Heinrich stadials further point to changes in Southern Ocean processes, potentially linked to a non-linear or threshold response to AMOC changes.

Interstadials. Temperature reconstructions from the North Greenland Ice Core Project (NGRIP) suggest that D–O events of the last glacial period are characterized by a mean temperature increase of 12 ± 2.6 °C over a few decades[14]. Each episode of abrupt Greenland warming during MIS 3 was associated with a reduction in Norwegian Sea sea-ice cover, the spring sea-ice edge shifting north of ~62°N (REFS[41,42]) and an abrupt 4–6 °C increase in North Atlantic summer SST[49,50].

This rapid North Atlantic temperature increase and sea-ice reduction is most likely due to the resumption of deep-ocean convection and, thus, NADW formation in the Nordic Seas[38,39,42,48,67,82,150]. Evidence for a consistently strong AMOC during interstadials also comes from low North Atlantic sedimentary $^{231}Pa/^{230}Th$ (REFS[10,68,117]) (FIG. 1a), the magnetic properties of North Atlantic sediment[151] and a high $[CO_3^{2-}]$ in the deep sub-Antarctic Atlantic Ocean[76].

A strong AMOC, similar to today's, is also consistent with the relatively warm and wet conditions over Europe and the Mediterranean region recorded during each interstadial[28,63,64,99–102,152–154]. In addition, Greenland and Antarctic ice-core records indicate that changes in the concentration of atmospheric CH_4 are tightly coupled to D–O variability[155–157]. As the dominant source of CH_4 to the atmosphere is anaerobic decomposition of organic matter in low-latitude wetlands[158], CH_4 variations indicate changes in the hydrological cycle of tropical and subtropical regions[155]. As northern tropical wetlands cover a larger area than their southern counterparts, the relatively high atmospheric CH_4 concentration recorded in high-resolution Antarctic ice cores during all interstadials of the last glacial period[159] (FIG. 1c) suggests a northward position of the ITCZ[160], consistent with a strong AMOC[112].

To summarize, palaeoproxy records from the Atlantic Basin indicate changes in oceanic circulation associated with D–O cycles of the last glacial period. In addition, there is substantial evidence for concurrent climatic variations in both proximal and distal regions, including southern high latitudes, which are consistent with AMOC changes. Together, the available observational records and numerical experiments indicate AMOC weakening during the transition to a D–O stadial, further AMOC weakening, or even shutdown, during Heinrich stadials and rapid AMOC strengthening towards interstadial conditions[10,38,39,117] (FIG. 4). However, what led to these AMOC variations?

Processes involved in D–O variability

Although the expression of D–O variability is relatively well constrained (except for details in relative phasing), particularly in the Atlantic region, and there is substantial evidence for its association with AMOC changes, the processes leading to this variability are still highly debated. No hypothesis can explain all inferred climate changes of the D–O and Heinrich continuum, raising questions regarding their origin. We address these questions in this section. Specifically, we consider whether the variability is internal to the atmosphere–ocean–sea-ice system[55–58] and whether changes in CO_2 concentration could trigger the transitions[60]. Moreover, we discuss whether ice-sheet discharges are needed to explain non-Heinrich stadials and whether the correspondence of Heinrich events with D–O stadials represents the phase locking of two separate oscillatory systems through, for example, stochastic resonance[161–163]. We also address questions regarding the processes involved in Heinrich events and the role of background conditions in AMOC stability.

Internal oscillations. Early studies hypothesized that D–O cycles were the result of a 'salt oscillator' (REFS[54,113]), whereby warm and wet conditions in the Northern Hemisphere during interstadials, associated with

increased continental ice-sheet melt, result in greater surface buoyancy in the North Atlantic, thus weakening NADW formation and the AMOC. Cold and dry conditions in the Northern Hemisphere during stadials, due to the southward shift of the ITCZ, would increase salinity in the tropical North Atlantic, thus strengthening the AMOC[164,165] (FIG. 5). Numerical experiments[55,57,164] and palaeoproxy records[67,81] provide support for the role of a North Atlantic salt oscillator during D–O cycles, highlighting the tight coupling between sea ice, North Atlantic salinity transport and NADW formation.

Internal millennial-scale AMOC variations have been simulated in coupled climate models[55–58,166–168], usually under specific boundary conditions. Some of these oscillations were initiated by stochastic atmospheric forcing[167,168] or stochastic changes in the Nordic Seas

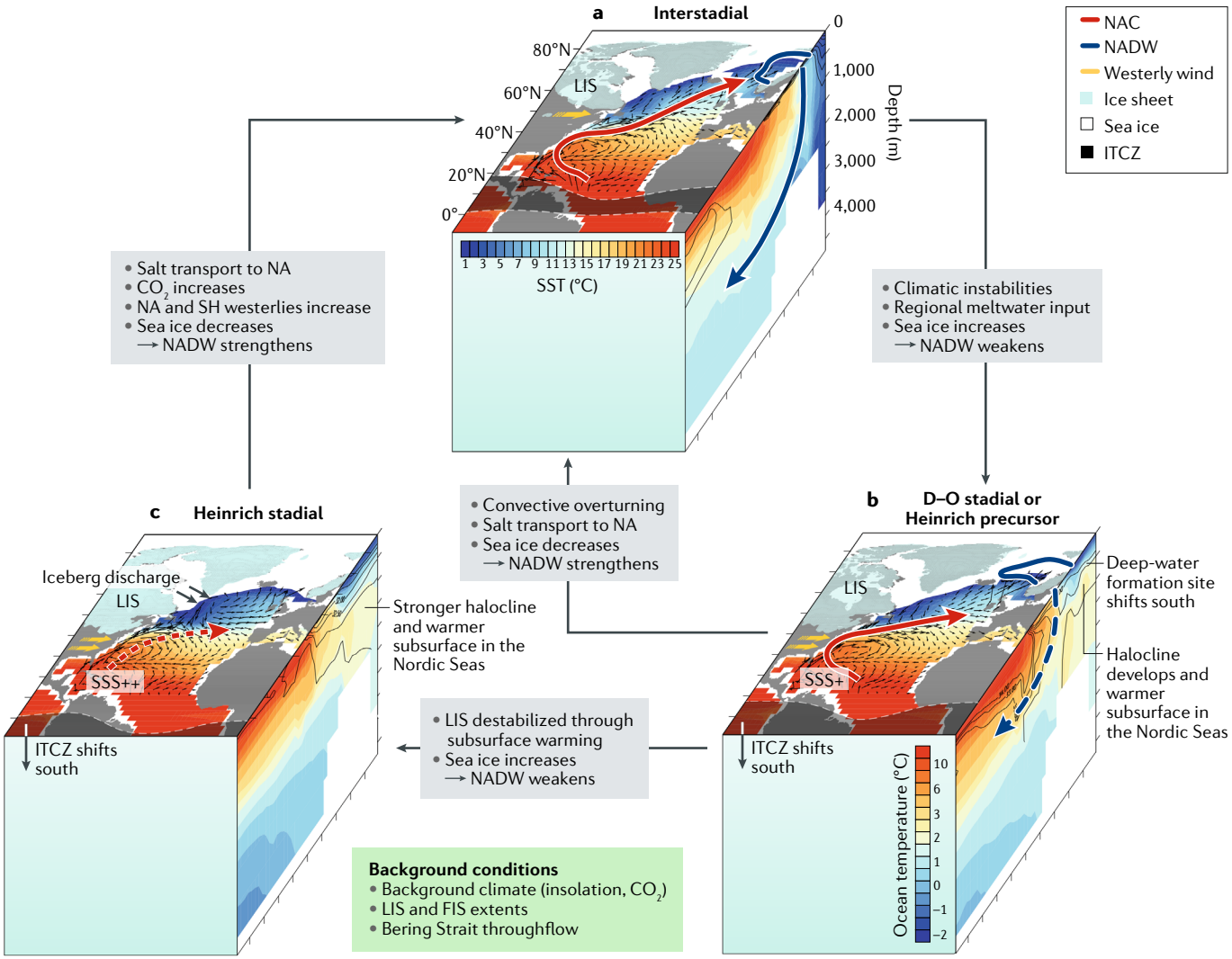

Fig. 5 | **Summary of interactions and feedbacks involved in D–O variability.** Schematic of an interstadial peak (panel **a**), a Dansgaard–Oeschger (D–O) stadial or Heinrich precursor (panel **b**) and a Heinrich stadial (panel **c**) showing the possible mechanisms leading to transitions. These schematics qualitatively illustrate the main climatic changes associated with D–O variability, taking into account the large uncertainties associated with quantitative estimates. On going from interstadials to D–O and Heinrich stadials, North Atlantic Deep Water (NADW) formation weakens, deep-water formation sites shift southward, sea-ice extent increases, the annual mean sea-surface temperature (SST) decreases and surface currents (black arrows) are modified, with, in particular, weakening of the North Atlantic Current (NAC). The subsurface temperature in the northern North Atlantic (NA) increases (the side panel shows the annual mean zonally averaged temperature in the Atlantic with respect to depth and latitude), while a stronger halocline develops (side panel contours). Warmer subsurface conditions could destabilize the Laurentide Ice Sheet (LIS) and lead to iceberg discharges in the Hudson Strait, which is characteristic of Heinrich events. As the Atlantic meridional overturning circulation (AMOC) weakens, the Intertropical Convergence Zone (ITCZ) shifts southward, increasing sea-surface salinity in the tropical Atlantic (SSS+). A possible southward extension of the LIS during stadials would intensify North Atlantic westerly winds (yellow arrows). Breakdown of the halocline through convective overturning or increased salt transport to the North Atlantic could lead to a stadial to interstadial transition. Stronger Northern Hemisphere westerlies (arising from LIS changes), Southern Hemisphere (SH) westerlies or increased atmospheric CO_2 concentration during Heinrich stadials could also contribute to AMOC reinvigoration towards an interstadial. Favourable background conditions for D–O variability to occur are indicated in green. FIS, Fennoscandian Ice Sheet.

overturning circulation[166]. In other models, the radiative balance led to sea-ice growth, and the associated North Atlantic salinity redistribution was sufficient to induce fairly rapid (≤500 years) cooling towards stadial conditions[55,57]. The interstadial transition is then initiated by a reorganization of the vertical thermohaline structure of the northern North Atlantic. On the basis of palaeoproxy records[42,67,81,82], it has been postulated that extensive perennial sea-ice cover and a strong halocline in the Nordic Seas during stadials would prevent heat transfer to the atmosphere and lead to an increase in heat content below the pycnocline (a depth of ~300 m; FIGS 3,5). Although a simple column model of the Nordic Seas has shown that this heat build-up below the pycnocline could induce convective overturning[169], the convective overturning in coupled models occurred in the northern North Atlantic, owing to either a northward salinity flux below the sea-ice lid[55] or the creation of a super polynya[57]. However, these simulated convective overturning events were obtained by adjusting the diapycnal diffusivity profiles of the ocean models[55,57]. Additional work is thus required to assess whether such convective overturning events could arise in the Nordic Seas under intermediate glacial conditions.

The cooling towards stadial conditions would potentially be slower and, thus, in better agreement with palaeorecords, if it involved the build-up of extensive ice shelves in the Labrador and/or Nordic Seas[170,171]. There is some observational support for the presence of fringing ice shelves around Greenland during the last glacial interval[172,173]. However, the current evidence suggests that Baffin Bay was not covered by a full ice shelf at the LGM and, thereby, perhaps also during MIS 3 (REF.[174]).

An outstanding challenge for models is to obtain D–O-like oscillations under only appropriate boundary conditions and forcings. Oscillatory behaviour under fixed boundary conditions has been observed in only a few modelling experiments[55–58], some of which used very specific boundary conditions, including pre-industrial Northern Hemisphere ice sheets, low obliquity (22°), low CO_2 concentration (≤217 ppm)[56,58,166] or LGM boundary conditions[55,57], that do not match those of MIS 3 when D–O variability was most prevalent.

Impact of atmospheric CO_2 changes on the AMOC. Heinrich stadials are associated with an increase in CO_2 concentration of up to ~20 ppm, followed by a millennial-scale 20–30 ppm decrease[46,141] (FIG. 1h). However, current records are unable to resolve significant CO_2 concentration changes during D–O stadials, and MIS 3 includes multi-millennial periods with D–O events but CO_2 changes of <10 ppm. A gradual CO_2 increase could lead to abrupt AMOC strengthening at the end of Heinrich stadials by decreasing the sea-ice cover in the North Atlantic either directly or through increased salt transport from the tropical to the North Atlantic[59,60,175]. This AMOC sensitivity to CO_2 changes seems to occur in models that display deep-water formation in the northern North Atlantic, south of Iceland. By contrast, models that simulate deep-water formation in the Nordic Seas display a much higher AMOC stability to changes in CO_2 under MIS 3 boundary conditions[176], potentially indicating that AMOC stability is dependent on the location and strength of deep-water formation.

Meltwater discharges and D–O stadials. $\delta^{18}O$ records from the Norwegian and Irminger Seas are consistent with decreases in sea-surface salinity (and, thus, halocline strengthening) occurring in phase with stadials[49,81], possibly due to melting and calving of the circum-North Atlantic ice sheets[177,178]. It is, however, unclear whether the magnitude of the associated meltwater input would have been sufficient to weaken the AMOC. Although the AMOC stability generally seems to be lower under intermediate glacial conditions than interglacial ones[38,39,60,179], only a few models are very close to the stability threshold[60,179]. However, changes in LIS height could have also directly affected the AMOC strength through changes in North Atlantic wind stress, thus lowering the stability threshold[59,60].

Calving of circum-North Atlantic ice sheets is supported by the presence of IRD layers in North Atlantic marine sediment cores during all D–O stadials[20,47,51]. Iceberg discharges require a marine ice-sheet boundary. The cold surface air and SSTs during stadials would have promoted marine ice-sheet expansion[177]. But with the stadial accumulation of heat below the halocline, these marine margins could have then become destabilized, with a resultant increase in iceberg discharges[178]. A complication for causal inference is that the presence of IRD also reflects, to an uncertain extent, enhanced preservation of icebergs, owing to colder near-surface ocean temperatures as they are advected to the marine core sites. Therefore, it has also been suggested that North Atlantic cooling preceded IRD deposition, thus implying that iceberg discharges could be a consequence and not a cause of stadials[20].

Although Nordic Seas sea ice, freshwater balance and, thus, stratification appear to have a key role in D–O variability, further work is needed to fully understand the underlying processes. In this regard, key questions to resolve are: what are the mechanisms involved specifically in Heinrich events and how do they relate to D–O cycles?

Processes leading to Heinrich events. From the mid-Pleistocene transition (~640 ka), Heinrich events are identified by thick layers of IRD originating from the Hudson Strait, thus indicating LIS discharges. Red Sea isotope records and fossil coral data suggest that Heinrich events could have been associated with a global mean sea-level rise of >15 m (REFS[36,180–182]). However, the amplitude and, especially, the timing of these potential sea-level variations are still uncertain[183]. Given the evidence for Hudson Strait provenance of IRD and substantial sea-level change, LIS dynamics have been proposed to explain Heinrich events[177].

The most prominent theories include a growth–purge mechanism (usually referred to as binge–purge), which involves free oscillations of the ice stream owing to build-up and subsequent purging of basal ice at the pressure melting point for ice streaming[184]. A numerical simulation performed with a coupled ice-sheet and simplified climate model[185] obtained multi-millennial oscillations with an associated change in LIS ice volume

equivalent to a sea-level change of 5–10 m. For this model, each Heinrich event was triggered by small-scale instabilities of the ice sheet at the mouth of the Hudson Strait. In addition, a comparison of ice-sheet models[186] found the growth–purge mechanism to be fairly robust across most participating models, with a strong dependence of ice-loss magnitude on the parameterization of the basal sliding rate and with periods in the 5–17-kyr range, depending on the model. This study also showed that the oscillations cease with higher temperatures, owing to sustained ice streaming.

Complementary theories have sought to more directly link LIS disintegration to climatic conditions or to elucidate the physical trigger mechanism that was idealized in previous studies[185]. Subsurface warming in the northern North Atlantic and Nordic Seas during AMOC weakening[67,81,115,187,188] could trigger iceberg discharges in the Hudson Strait through two mechanisms: the break-up of an ice shelf on the Labrador Sea or direct retreat of marine-terminated LIS. The first mechanism assumes that stadial conditions would enable the formation of a large ice shelf at the mouth of the Hudson Strait, in part, through buttressing and the suppression of submarine convection by adjacent sea ice[189], especially land-fast ice[190]. This ice shelf would be vulnerable to intrastadial climate ameliorations[172,174] and/or subsurface warming resulting from a weaker AMOC[115,187,191,192], thus inducing catastrophic ice-shelf break-up and a loss of buttressing of the Hudson Strait ice stream. To date, however, it is unclear whether a substantial ice shelf developed at the mouth of the Hudson Strait during glacial times. Even without the presence of a large terminal ice shelf, the Hudson Strait ice stream was marine terminating and, thus, subject to potentially high melt from subsurface ocean warming, which could facilitate fast marine margin retreat. If such a subsurface warming also extended into the Greenland and Nordic Seas, and at a depth where it could affect the marine-terminated ice sheets or ice shelves, as inferred from some climate model experiments[84,115,135,188] (FIG. 3), then it could lead to concurrent discharges of the European and Greenland ice sheets[178,193]. Isostatic adjustment of the sill elevation at the mouth of the Hudson Strait could also control the contact between warm subsurface waters and the calving face and, thus, modulate LIS discharges[194]. These hypotheses can, therefore, explain the occurrence of Heinrich events during stadials[20], as well as the occurrence of simultaneous disintegration events from other circum-Atlantic ice sheets through subsurface warming. However, although there is some observational evidence for subsurface warming of the Norwegian Sea[67,81,82] and northwestern Atlantic[115] during Heinrich stadials, additional studies are needed to constrain the magnitude, location and depth of this warming.

Changes in the southern extent or height of the LIS could also directly affect North Atlantic sea-ice concentration, temperature[195–197] and the AMOC[59] by modulating the strength and position of the North Atlantic westerlies. There is some evidence for a dynamic LIS during MIS 3: radiocarbon dates and relative sea-level constraints are consistent with a LIS southern margin proximal to the southern edge of Hudson Bay (~51°N) during the interstadial at 46.7 ka, followed by a fast southward advance to ~44°N during Heinrich stadial 4 and subsequent retreat[198]. Thus, a dynamic LIS may have modulated the AMOC strength, either through atmospheric steering or freshwater delivery to the North Atlantic (as the southern extent would determine whether central LIS meltwater was routed southward to the Gulf of Mexico or eastward to the North Atlantic)[199].

Background conditions and AMOC stability. Although D–O variability stricto sensu is suppressed during interglacial times owing to the lack of large circum-Atlantic ice sheets, recent palaeoproxy records have highlighted periods of weaker AMOC during several interglacial periods[200–202]. The processes leading to these AMOC weakenings are poorly constrained, but some of these weakenings could be due to meltwater discharges from the Greenland ice sheet[203]. Nevertheless, during interglacial times, the AMOC seems to be in a relatively stable strong state, and the AMOC perturbations are of lower magnitude than those during glacial periods.

The prevalence of D–O variability during intermediate glacials indicates that background conditions, including CO_2 concentration, the size of Northern Hemisphere continental ice sheets and the associated sea level, most likely influence the AMOC stability. Owing to the presence of Northern Hemisphere ice sheets, colder conditions in the North Atlantic and larger sea-ice coverage under glacial conditions, the AMOC transition threshold during intermediate glacial states seems to be lower than during interglacials — that is, a smaller perturbation is needed to significantly increase the sea-ice coverage and weaken the AMOC[38,39,179,204]. The closure of the Bering Strait, with its shallow sill depth at ~50 m below sea level, further lowers the perturbation threshold[205], owing to its influence on the North Atlantic freshwater budget. On the one hand, the closure of the Bering Strait strengthens the AMOC by hampering the flow of low-salinity Pacific waters towards the Arctic[205,206]. On the other hand, when the Bering Strait is closed, freshwater pulses would lead to persistent low-salinity anomalies in the North Atlantic, as they cannot be flushed out through the Bering Strait[207]. In addition, numerical experiments suggest that the formation of NPIW could strengthen when the AMOC weakens considerably and the Bering Strait is closed[143,146]. This change in the NPIW could lead to warmer and wetter conditions over North America[208] (FIG. 5) and, thus, affect the LIS mass balance.

Using a zonally averaged multi-basin model, it was suggested that a weak (stadial) AMOC state with deep convection south of Iceland could be stable under glacial conditions[38]. However, modelling studies performed with coupled climate models under intermediate glacial background conditions found the AMOC to be bistable, shifting between a weak state and a strong state following small perturbations to the system[59,60,179], or with a stable strong AMOC state[176] and temporarily stable AMOC off state following meltwater perturbations[39]. It is, thus, likely that both the stability of the AMOC is lower and the perturbations to the system are greater during intermediate glacial than interglacial states, owing to the

presence of larger Northern Hemisphere ice sheets. As developed further below, perturbations to the system are not restricted to meltwater input but also include centennial-scale changes in Northern Hemisphere ice sheets, CO_2 concentration and subsurface warming.

Finally, palaeoproxy records suggest that the AMOC was shallower[209,210] and potentially weaker[211–213] during the LGM, whereas most of the Paleoclimate Modelling Intercomparison Project phases 3 and 4 (PMIP3 and PMIP4) LGM experiments suggest that the AMOC was as strong as during interglacials[214,215]. This discrepancy between the AMOC state inferred from proxy records and modelling suggests that either the glacial perturbations (in this case, most likely meltwater input) are poorly constrained or that deep-water formation does not occur at the 'right place' in the models, making them overly sensitive to changes in North Atlantic wind stress. Through strengthening of the North Atlantic wind stress, a large LIS could lead to a strong AMOC[216], which would likely be more stable and less prone to internal oscillations[38,56,58,176]. Strong westerly wind stress over the North Atlantic indeed strengthens the subpolar gyre, the salt transport in the Irminger current and the eddy salt flux to the centre of the gyre, which would favour NADW formation[217,218]. However, the importance of this process is likely dependent on the location of deep-water formation (that is, in the Labrador or Nordic Seas). Indeed, in contrast to recent estimates[1], in some historical CMIP5 simulations, deep water primarily formed in the Labrador Sea[219].

Synthesis and proposed oscillatory system

Although a complete explanation for D–O variability remains elusive, a tentative scheme can be advanced. As there is strong coupling between sea-ice formation, deep-ocean convection in the Nordic Seas and the AMOC, a small perturbation in the heat or salt flux in the Nordic Seas, such as increased meltwater run-off from circum-Atlantic ice sheets, a decrease in CO_2 or other climatic instabilities could lead to sea-ice advance[220], a southward shift of the convection site[221] and AMOC weakening, thus leading to a stadial (FIG. 5b).

AMOC weakening would reduce the transport of cold surface and subsurface waters through the Denmark Strait overflow[1,116]. This change in oceanic circulation, associated with increased sea-ice cover, would lead to subsurface warming in the Nordic Seas[81,135] and the northwestern Atlantic[115,188] (FIG. 3). In turn, northwestern Atlantic subsurface warming could have triggered the disintegration of a Labrador Sea ice shelf[115,191] or the retreat of the Hudson Strait ice stream[194], thus leading to the Hudson Strait iceberg discharges characteristic of Heinrich events. Recurrent episodes of AMOC weakening and subsurface warming would trigger a Heinrich event only when ice-shelf or ice-sheet conditions permitted (depending on, for example, ice-sheet thickness and basal ice temperature), thus providing a plausible explanation for the link between D–O cyclicity and Heinrich events.

Further AMOC weakening during a Heinrich stadial is linked to sea-ice advance and the lack of sustained deep-ocean convection. The transition to an interstadial would arise from an increase in surface salinity in the northern North Atlantic and/or a decrease in sea-ice extent. The proposed mechanisms are not mutually exclusive and include convective overturning in the Nordic Seas, brought about by the subsurface warming[81]; increased transport of low-latitude salty surface waters to the North Atlantic[164], potentially amplified by a strengthening of the westerlies over the North Atlantic owing to an increase in LIS height; and/or a gradual CO_2 increase[59,60] (FIG. 5a). Finally, Southern Ocean processes could also contribute to reinvigoration of the AMOC. Through enhanced Southern Ocean upwelling and Ekman transport of Southern Ocean waters to the Atlantic, a strengthening of Southern Hemisphere westerlies (due to a southward shift of the ITCZ) during Heinrich stadials could strengthen the AMOC by up to 4 Sv (REFS[222,223]). However, eddy compensation in the Southern Ocean could substantially reduce the impact of Southern Hemisphere winds on the AMOC[224]. A bipolar ocean see-saw, NADW–Antarctic Bottom Water (AABW), could also strengthen NADW formation after episodes of deep-ocean convection in the Southern Ocean during Heinrich stadials, owing to density differences between NADW and AABW[225,226].

A self-sustained oscillatory framework. On the basis of the evidence for a 1–2-kyr periodicity of D–O cycles[23,31,35,49,227,228], the occurrence of stochastic resonance, both 'autonomous' (purely internal to the ocean–sea-ice–atmosphere system) and 'non-autonomous' (arising from the influence of an external, possibly periodic, forcing), has been proposed[161–163]. However, the numerical models first used to investigate the role of stochastic resonance in D–O variability were box models, lacking important processes and feedbacks. As detailed above, improvements in climate-modelling capacity, as well as additional and more detailed palaeorecords, now provide a clearer picture of the processes at play.

We thus propose that the D–O variability could be explained by a self-sustained oscillatory framework of the coupled climate–ice-sheet system, which would be characterized by a relatively low stability of the AMOC in its strong state under intermediate glacial conditions. Small perturbations (for example, centennial-scale changes in the northern North Atlantic freshwater balance, CO_2 or wind) could then lead to AMOC weakening and an associated rapid Northern Hemisphere sea-ice advance into a stadial. This AMOC weakening and sea-ice advance would induce climatic changes, including subsurface warming in the northern North Atlantic and a southward shift of the ITCZ, with the latter leading to saltier conditions in the tropical North Atlantic. On a multi-centennial timescale, these climatic changes act as negative feedback on the AMOC and sea-ice changes, thus leading to AMOC recovery and rapid sea-ice retreat into an interstadial. Depending on the state of the LIS, and possibly the surrounding ice shelves, the initial AMOC weakening and associated climatic changes could trigger the LIS discharges characteristic of Heinrich events, which act as a positive feedback, amplifying the AMOC weakening and sea-ice advance. An AMOC off state, with enhanced NPIW and AABW

formation, could then be marginally stable. However, the larger amplitude of the anomalies generated during Heinrich stadials, particularly North Atlantic subsurface warming, changes in LIS extent, strengthening of Southern Hemisphere westerlies and CO_2 increase, would have the potential to trigger AMOC recovery and even overshoot (FIGS 1,5). Such an AMOC overshoot and associated North Atlantic surface warming could then push the system back towards stadial conditions.

From this synthesis of the proposed D–O sequence tentatively emerges an oscillatory system characterized by self-sustained centennial-scale to millennial-scale variations in the ocean–sea-ice–atmosphere system that resonate with (and help to trigger) multi-millennial scale variations in marine-based ice sheets, potentially through ice-shelf-related dynamical instabilities. The expression of this oscillatory system would, in theory, be amplified or damped (turned on or off) according to the background climate state (for example, temperature, salinity and wind stress), which is also linked to ice volume. The preponderance of D–O variability during intermediate glacial states indeed suggests a dependence on background conditions, including any or all of the following: the presence of the LIS, but of moderate size so as not to induce strong North Atlantic westerly wind stress, such as prevails at the LGM[214,216]; relatively high boreal summer insolation at high northern latitudes, leading to summer melt of circum-Atlantic ice sheets; and sea-level modulation (if not closure) of the Bering Strait throughflow, which would affect the North Atlantic freshwater budget and AMOC stability[205,206]. However, it should be noted that D–O cycles 4 and 3 occurred when the LIS was large and the summer insolation at high northern latitudes was moderate.

Summary and outlook

Glacial periods of the Pleistocene, and particularly glacial states with an intermediate Northern Hemisphere ice-sheet volume, are characterized by millennial-scale climate variability[23,25–27,31,33]. This D–O variability involves variations in AMOC strength and Nordic Seas sea ice, thus leading to surface temperature changes of opposite signs and asynchronous timing in both hemispheres[22]. The climatic expression of D–O variability is fairly well constrained in the Atlantic region and surrounding land masses, but the knowledge of its expression in other regions is more limited, owing to a lack of high-resolution proxy records, issues with age constraints and interpretations, as well as a lack of knowledge on the oceanic and atmospheric teleconnections arising from a weaker AMOC and associated cooler North Atlantic.

The sequence of events that led to D–O climatic variability is still highly debated. Several mechanisms have been put forward to explain the D–O variability; however, none can currently replicate all the characteristics of D–O cycles, including their preponderance during intermediate glacial states. Here, we propose a self-sustained oscillatory model of the climate–ice-sheet system, modulated by background climatic conditions, to synthesize observations and current understanding of the underlying processes. In this self-sustained oscillatory conceptual framework centred on AMOC and Nordic Seas sea-ice changes, which feed back on each other, the climatic, CO_2 and ice-sheet changes occurring during stadials provide a negative feedback on the AMOC and Nordic Seas sea-ice cover, thus leading to the AMOC reinvigoration to interstadial conditions (FIG. 5b), and vice versa. D–O variability would not be a simple response to meltwater fluxes. Instead, D–O cyclicity would represent an emergent phenomenon rooted in the ocean–sea-ice–atmosphere system and linked to ice-sheet dynamics (and, therefore, Heinrich events) through the impact of AMOC changes on ice-shelf stability and/or ice streaming, as well as through potential positive feedbacks from meltwater delivery on AMOC strength. This framework complements the previously suggested AMOC hystereses as a function of meltwater input[8], LIS or CO_2 changes[59,60], as it acknowledges that the AMOC does not only respond to but also influences the climate, ice sheets and the carbon cycle.

The principal challenge in further developing these theories is that current Earth system models do not include all necessary components (for example, biogeochemistry, ice shelves, ice-sheet dynamics), inadequately represent important processes or cannot be integrated long enough under intermediate glacial conditions to simulate self-sustained D–O cycles. NADW formation in climate models is highly parameterized and not well constrained by observations, so there is little confidence in simulated changes in the strength and location of NADW formation in response to climate change, both past and future. Owing to relatively long integration times necessary to understand the processes involved in D–O variability, numerical experiments have been performed with simpler or relatively coarse-resolution climate models that do not include ice sheets and/or do not adequately resolve relevant boundary currents and key marine sills. Given the complexity of the oceanic circulation in the North Atlantic and Nordic Seas regions, and the central role of mesoscale eddies in salt and heat transport, the processes at play could be better constrained by performing numerical experiments with higher-resolution coupled climate models. Coupled climate–ice-sheet model simulations of past glacial periods are starting to emerge[197] but need to be expanded to help in the understanding of the interaction between ice-sheet, ice-shelf, sea-ice and AMOC variations. Additional observational data on the magnitude and timing of glacioeustatic changes in sea levels and Northern Hemisphere ice sheets, and their relative timing with respect to D–O variability, are needed to better constrain the role of changes in ice-sheet volume and associated meltwater input into the ocean. Owing to the strong coupling between sea-ice and deep-water formation, additional records of past millennial-scale changes in sea-ice cover in the Nordic Seas and northern North Atlantic are required. Finally, as subsurface warming in the northern North Atlantic during stadials likely had an important role in triggering D–O and Heinrich events, additional ocean-interior temperature records and process studies are needed to quantify the magnitude, location and depth of this potential warming.

Past AMOC changes suggest that the AMOC might be less stable than currently simulated by climate models and/or that the range of processes affecting the buoyancy and dynamics of the North Atlantic and Nordic Seas might be larger than classically thought. As anthropogenic emissions of carbon accumulate in the atmosphere, run-off from the Greenland ice sheet will increase and the Arctic sea-ice extent will continue to decline. These factors are likely to weaken the AMOC, with important implications for the climate, cryosphere and global carbon cycle.

Published online: 03 November 2020

1. Lozier, M. S. et al. A sea change in our view of overturning in the subpolar North Atlantic. *Science* **363**, 516–521 (2019).
2. Rahmstorf, S. et al. Exceptional twentieth-century slowdown in Atlantic Ocean overturning circulation. *Nat. Clim. Change* **5**, 475–480 (2015).
3. Marchitto, T. M. & deMenocal, P. B. Late Holocene variability of upper North Atlantic deep water temperature and salinity. *Geochem. Geophys. Geosyst.* **4**, 1100 (2003).
4. Thornalley, D. et al. Anomalously weak Labrador Sea convection and Atlantic overturning during the past 150 years. *Nature* **556**, 227–230 (2018).
5. Kobashi, T. et al. Volcanic influence on centennial to millennial Holocene Greenland temperature change. *Sci. Rep.* **7**, 1441 (2017).
6. Stommel, H. Thermohaline convection with two stable regimes of flow. *Tellus* **13**, 224–230 (1961).
7. Reintges, A., Martin, T., Latif, M. & Keenlyside, N. S. Uncertainty in twenty-first century projections of the Atlantic meridional overturning circulation in CMIP3 and CMIP5 models. *Clim. Dyn.* **49**, 1495–1511 (2017).
8. Hofmann, M. & Rahmstorf, S. On the stability of the Atlantic meridional overturning circulation. *Proc. Natl Acad. Sci. USA* **106**, 20584–20589 (2009).
9. Valdes, P. Built for stability. *Nat. Geosci.* **4**, 414–416 (2011).
10. Henry, L. et al. North Atlantic ocean circulation and abrupt climate change during the last glaciation. *Science* **353**, 470–474 (2016).
11. Dansgaard, W. et al. A new Greenland deep ice core. *Science* **218**, 1273–1277 (1982).
12. Dansgaard, W., Johnsen, S. & Clausen, H. Evidence for general instability of past climate from a 250-kyr ice-core record. *Nature* **364**, 218–220 (1993).
13. North Greenland Ice Core Project members. High-resolution record of the Northern Hemisphere climate extending into the last interglacial period. *Nature* **431**, 147–151 (2004).
Presents a highly resolved record of D–O variability in a Greenland ice core.
14. Kindler, P. et al. Temperature reconstruction from 10 to 120 kyr b2k from the NGRIP ice core. *Clim. Past* **10**, 887–902 (2014).
15. Heinrich, H. Origin and consequences of cyclic ice rafting in the northeast Atlantic Ocean during the past 130,000 years. *Quat. Res.* **29**, 142–152 (1988).
16. Bond, G., Heinrich, H., Broecker, W. & Labeyrie, L. Evidence of massive discharges of icebergs into the North Atlantic during the last glacial period. *Nature* **360**, 245–249 (1992).
17. Bond, G. Correlations between climate records from North Atlantic sediments and Greenland ice. *Nature* **365**, 143–147 (1993).
Highlights D–O oscillations in marine sediment cores from the North Atlantic and establishes a link to variations in Greenland ice-core $\delta^{18}O$ records.
18. Hemming, S. Heinrich events: Massive late Pleistocene detritus layers of the North Atlantic and their global climate imprint. *Rev. Geophys.* **42**, RG1005 (2004).
19. Sánchez-Goñi, M. & Harrison, S. Millennial-scale climate variability and vegetation changes during the last glacial: concepts and terminology. *Quat. Sci. Rev.* **29**, 2823–2827 (2010).
20. Barker, S. et al. Icebergs not the trigger for North Atlantic cold events. *Nature* **520**, 333–336 (2015).
21. Naafs, B., Hefter, J. & Stein, R. Millennial-scale ice rafting events and Hudson Strait Heinrich(-like) Events during the late Pliocene and Pleistocene: a review. *Quat. Sci. Rev.* **80**, 1–28 (2013).
22. Barker, S. et al. 800,000 years of abrupt climate variability. *Science* **334**, 347–351 (2011).
23. Oppo, D. W., McManus, J. F. & Cullen, J. L. Abrupt climate events 500,000 to 340,000 years ago: evidence from subpolar North Atlantic sediments. *Science* **279**, 1335–1338 (1998).
24. Raymo, M., Ganley, K., Carter, S., Oppo, D. & McManus, J. Millennial-scale climate instability during the early Pleistocene epoch. *Nature* **392**, 699–702 (1998).
25. McManus, J. F., Oppo, D. W. & Cullen, J. L. A 0.5-million-year record of millennial-scale climate variability in the North Atlantic. *Science* **283**, 971–975 (1999).
Provides evidence for millennial-scale climatic variability in the North Atlantic over the past 500,000 years and, particularly, during intermediate glacial states.
26. Martrat, B. et al. Four climate cycles of recurring deep and surface water destabilizations on the Iberian margin. *Science* **317**, 502–507 (2007).
27. Hodell, D. A., Channell, J. E. T., Curtis, J. H., Romero, O. E. & Röhl, U. Onset of "Hudson Strait" Heinrich events in the eastern North Atlantic at the end of the middle Pleistocene transition (~640 ka)? *Paleoceanography* **23**, PA4218 (2008).
28. Margari, V. et al. The nature of millennial-scale climate variability during the past two glacial periods. *Nat. Geosci.* **3**, 127–131 (2010).
29. Bailey, I. et al. Flux and provenance of ice-rafted debris in the earliest Pleistocene sub-polar North Atlantic Ocean comparable to the last glacial maximum. *Earth Planet. Sci. Lett.* **341-344**, 222–233 (2012).
30. Obrochta, S. P. et al. Climate variability and ice-sheet dynamics during the last three glaciations. *Earth Planet. Sci. Lett.* **406**, 198–212 (2014).
31. Birner, B., Hodell, D. A., Tzedakis, P. C. & Skinner, L. C. Similar millennial climate variability on the Iberian margin during two early Pleistocene glacials and MIS 3. *Paleoceanography* **31**, 203–217 (2016).
32. Hodell, D. A. & Channell, J. E. T. Mode transitions in Northern Hemisphere glaciation: co-evolution of millennial and orbital variability in Quaternary climate. *Clim. Past* **12**, 1805–1828 (2016).
33. Rodrigues, T. et al. A 1-Ma record of sea surface temperature and extreme cooling events in the North Atlantic: a perspective from the Iberian Margin. *Quat. Sci. Rev.* **172**, 118–130 (2017).
34. Shackleton, N. Oxygen isotopes, ice volume and sea level. *Quat. Sci. Rev.* **6**, 183–190 (1987).
35. Schulz, M., Berger, W., Sarnthein, M. & Grootes, P. Amplitude variations of 1470-year climate oscillations during the last 100,000 years linked to fluctuations of continental ice mass. *Geophys. Res. Lett.* **22**, 3385–3388 (1999).
36. Siddall, M., Rohling, E. J., Thompson, W. G. & Waelbroeck, C. Marine isotope stage 3 sea level fluctuations: data synthesis and new outlook. *Rev. Geophys.* **46**, RG4003 (2008).
37. Kawamura, K. et al. State dependence of climatic instability over the past 720,000 years from Antarctic ice cores and climate modeling. *Sci. Adv.* **3**, e1600446 (2017).
38. Ganopolski, A. & Rahmstorf, S. Rapid changes of glacial climate simulated in a coupled climate model. *Nature* **409**, 153–158 (2001).
Reports modelling results that suggest that D–O variability is due to AMOC changes, and introduces the idea of the AMOC flickering between three states.
39. Menviel, L., Timmermann, A., Friedrich, T. & England, M. Hindcasting the continuum of Dansgaard–Oeschger variability: mechanisms, patterns and timing. *Clim. Past* **10**, 63–77 (2014).
40. Lynch-Stieglitz, J. The Atlantic meridional overturning circulation and abrupt climate change. *Annu. Rev. Mar. Sci.* **9**, 83–104 (2017).
41. Hoff, U., Rasmussen, T., Stein, R., Ezat, M. & Fahl, K. Sea ice and millennial-scale climate variability in the Nordic Seas 90 kyr to present. *Nat. Commun.* **7**, 12247 (2016).
42. Sadatzki, H. et al. Sea ice variability in the southern Norwegian Sea during glacial Dansgaard-Oeschger climate cycles. *Sci. Adv.* **5**, eaau6174 (2019).
43. Wang, Y. et al. A high-resolution absolute-dated Late Pleistocene monsoon record from Hulu Cave, China. *Science* **294**, 2345–2348 (2001).
44. EPICA Community Members. One-to-one coupling of glacial climate variability in Greenland and Antarctica. *Nature* **444**, 195–198 (2006).
45. Deplazes, G. et al. Links between tropical rainfall and North Atlantic climate during the last glacial period. *Nat. Geosci.* **6**, 213–217 (2013).
46. Ahn, J. & Brook, E. Siple Dome ice reveals two modes of millennial CO_2 change during the last ice age. *Nat. Commun.* **5**, 3723 (2014).
47. Bond, G. & Lotti, R. Iceberg discharges into the North Atlantic on millennial time scales during the last glaciation. *Science* **267**, 1005–1010 (1995).
48. Dokken, T. & Jansen, E. Rapid changes in the mechanism of ocean convection during the last glacial period. *Nature* **401**, 458–461 (1999).
49. van Kreveld, S. et al. Potential links between surging ice sheets, circulation changes, and the Dansgaard-Oeschger cycles in the Irminger Sea, 60–18 kyr. *Paleoceanography* **15**, 425–442 (2000).
50. Dickson, A. J., Austin, W. E. N., Hall, I. R., Maslin, M. A. & Kucera, M. Centennial-scale evolution of Dansgaard-Oeschger events in the northeast Atlantic Ocean between 39.5 and 56.5 ka BP. *Paleoceanography* **23**, PA3206 (2008).
51. Hodell, D., Evans, H., Channell, J. & Curtis, J. Phase relationships of North Atlantic ice-rafted debris and surface-deep climate proxies during the last glacial period. *Quat. Sci. Rev.* **29**, 3875–3886 (2010).
52. Manabe, S. & Stouffer, R. Simulation of abrupt climate change induced by freshwater input to the North Atlantic Ocean. *Nature* **378**, 165–167 (1995).
53. Stouffer, R. et al. Investigating the causes of the response of the thermohaline circulation to past and future climate changes. *J. Clim.* **19**, 1365–1387 (2006).
54. Broecker, W. S., Bond, G., Klas, M., Bonani, G. & Wolfli, W. A salt oscillator in the glacial Atlantic? 1. The concept. *Paleoceanogr. Paleoclimatol.* **5**, 469–477 (1990).
55. Peltier, W. R. & Vettoretti, G. Dansgaard-Oeschger oscillations predicted in a comprehensive model of glacial climate: A "kicked" salt oscillator in the Atlantic. *Geophys. Res. Lett.* **41**, 7306–7313 (2014).
56. Brown, N. & Galbraith, E. D. Hosed vs. unhosed: interruptions of the Atlantic meridional overturning circulation in a global coupled model, with and without freshwater forcing. *Clim. Past* **12**, 1663–1679 (2016).
57. Vettoretti, G. & Peltier, W. R. Thermohaline instability and the formation of glacial North Atlantic super polynyas at the onset of Dansgaard-Oeschger warming events. *Geophys. Res. Lett.* **43**, 5336–5344 (2016).
58. Klockmann, M., Mikolajewicz, U. & Marotzke, J. Two AMOC states in response to decreasing greenhouse gas concentrations in the coupled climate model MPI-ESM. *J. Clim.* **31**, 7969–7984 (2018).
59. Zhang, X., Lohmann, G., Knorr, G. & Purcell, C. Abrupt glacial climate shifts controlled by ice sheet changes. *Nature* **512**, 290–294 (2014).
Shows that slow and moderate changes in LIS height or CO_2 concentration can trigger abrupt AMOC changes in a fully coupled climate model.
60. Zhang, X., Knorr, G., Lohmann, G. & Barker, S. Abrupt North Atlantic circulation changes in response to gradual CO_2 forcing in a glacial climate state. *Nat. Geosci.* **10**, 518–523 (2017).
61. Wolff, E., Chappellaz, J., Blunier, T., Rasmussen, S. & Svensson, A. Millennial-scale variability during the last glacial: the ice core record. *Quat. Sci. Rev.* **29**, 2828–2838 (2010).
62. Allen, J. R. M. et al. Rapid environmental changes in southern Europe during the last glacial period. *Nature* **400**, 740–743 (1999).
63. Genty, D. et al. Precise dating of Dansgaard–Oeschger climate oscillations in western Europe from stalagmite data. *Nature* **421**, 833–837 (2003).
64. Margari, V., Gibbard, P., Bryant, C. & Tzedakis, P. Character of vegetational and environmental changes in southern Europe during the last glacial period; evidence from Lesvos Island, Greece. *Quat. Sci. Rev.* **28**, 1317–1339 (2009).
65. Cacho, I. et al. Dansgaard-Oeschger and Heinrich event imprints in Alboran Sea paleotemperatures. *Paleoceanography* **14**, 698–705 (1999).

66. Martrat, B. et al. Abrupt temperature changes in the Western Mediterranean over the past 250,000 years. *Science* **306**, 1762–1765 (2004).
67. Rasmussen, T. L. & Thomsen, E. The role of the North Atlantic Drift in the millennial timescale glacial climate fluctuations. *Palaeogeogr. Palaeoclimatol. Palaeoecol.* **210**, 101–116 (2004).
68. Böhm, E. et al. Strong and deep Atlantic meridional overturning circulation during the last glacial cycle. *Nature* **517**, 73–76 (2015).
69. Burckel, P. et al. Atlantic Ocean circulation changes preceded millennial tropical South America rainfall events during the last glacial. *Geophys. Res. Lett.* **42**, 411–418 (2015).
70. Keigwin, L. D. & Boyle, E. A. Surface and deep ocean variability in the northern Sargasso Sea during marine isotope stage 3. *Paleoceanography* **14**, 164–170 (1999).
71. Shackleton, N., Hall, M. & Vincent, E. Phase relationships between millennial-scale events 64,000–24,000 years ago. *Paleoceanography* **15**, 565–569 (2000).
72. Skinner, L. C. & Elderfield, H. Rapid fluctuations in the deep North Atlantic heat budget during the last glacial period. *Paleoceanography* **22**, PA1205 (2007).
73. Lynch-Stieglitz, J. et al. Muted change in Atlantic overturning circulation over some glacial-aged Heinrich events. *Nat. Geosci.* **7**, 144–150 (2014).
74. Piotrowski, A. M., Goldstein, S. L., Hemming, S. R. & Fairbanks, R. G. Temporal relationships of carbon cycling and ocean circulation at glacial boundaries. *Science* **307**, 1933–1938 (2005).
75. Piotrowski, A., Goldstein, S., Hemming, S. R., Fairbanks, R. & Zylberberg, D. Oscillating glacial northern and southern deep water formation from combined neodynium and carbon isotopes. *Earth Planet. Sci. Lett.* **272**, 394–405 (2008).
76. Gottschalk, J. et al. Abrupt changes in the southern extent of North Atlantic Deep Water during Dansgaard–Oeschger events. *Nat. Geosci.* **8**, 950–954 (2015).
77. Trenberth, K. & Caron, J. Estimates of meridional atmosphere and ocean heat transports. *J. Clim.* **14**, 3433–3443 (2001).
78. Johns, W. E. et al. Continuous, array-based estimates of Atlantic Ocean heat transport at 26.5°N. *J. Clim.* **24**, 2429–2449 (2011).
79. Kageyama, M. et al. Climatic impacts of fresh water hosing under Last Glacial Maximum conditions: a multi-model study. *Clim. Past* **9**, 935–953 (2013).
80. Li, C., Battisti, D., Schrag, D. & Tziperman, E. Abrupt climate shifts in Greenland due to displacements of the sea ice edge. *Geophys. Res. Lett.* **32**, L19702 (2005).
81. Dokken, T., Nisancioglu, K., Li, C., Battisti, D. & Kissel, C. Dansgaard-Oeschger cycles: Interactions between ocean and sea ice intrinsic to the Nordic seas. *Paleoceanography* **28**, 491–502 (2013).
Presents observational evidence for the expression of D–O variability in the Nordic Seas, highlighting the possibility of the occurrence of convective overturning events.
82. Ezat, M. M., Rasmussen, T. L. & Groeneveld, J. Persistent intermediate water warming during cold stadials in the southeastern Nordic seas during the past 65 ky. *Geology* **42**, 663–666 (2014).
83. Müller, J. & Stein, R. High-resolution record of late glacial and deglacial sea ice changes in Fram Strait corroborates ice–ocean interactions during abrupt climate shifts. *Earth Planet. Sci. Lett.* **403**, 446–455 (2014).
84. He, C. et al. North Atlantic subsurface temperature response controlled by effective freshwater input in "Heinrich" events. *Earth Planet. Sci. Lett.* **539**, 116247 (2020).
85. Trenberth, K. E. & Fasullo, J. T. Atlantic meridional heat transports computed from balancing Earth's energy locally. *Geophys. Res. Lett.* **44**, 1919–1927 (2017).
86. Berger, W. & Wefer, G. *The South Atlantic* (Springer, 1996).
87. Schmittner, A., Saenko, O. & Weaver, A. Coupling of the hemispheres in observations and simulations of glacial climate change. *Quat. Sci. Rev.* **22**, 659–671 (2003).
88. Stocker, T. F. & Johnsen, S. J. A minimum thermodynamic model for the bipolar seesaw. *Paleoceanography* **18**, 1087 (2003).
89. Barker, S. & Diz, P. Timing of the descent into the last Ice Age determined by the bipolar seesaw. *Paleoceanography* **29**, 489–507 (2014).
90. Gottschalk, J., Skinner, L. C. & Waelbroeck, C. Contribution of seasonal sub-Antarctic surface water variability to millennial-scale changes in atmospheric CO_2 over the last deglaciation and Marine Isotope Stage 3. *Earth Planet. Sci. Lett.* **411**, 87–99 (2015).
91. Gottschalk, J. et al. Southern Ocean link between changes in atmospheric CO_2 levels and northern-hemisphere climate anomalies during the last two glacial periods. *Quat. Sci. Rev.* **230**, 106067 (2020).
92. Kaiser, J., Lamy, F. & Hebbeln, D. A 70-kyr sea surface temperature record off Southern Chile. *Paleoceanography* **20**, PA4009 (2005).
93. Pahnke, K., Zahn, R., Elderfield, H. & Schulz, M. 340,000-year centennial-scale marine record of Southern Hemisphere climatic oscillation. *Science* **301**, 948–952 (2003).
94. Caniupán, M. et al. Millennial-scale sea surface temperature and Patagonian Ice Sheet changes off southernmost Chile (53°S) over the past ~60 kyr. *Paleoceanography* **26**, PA3221 (2011).
95. Blunier, T. & Brook, E. Timing of millennial-scale climate change in Antarctica and Greenland during the last glacial period. *Science* **291**, 109–112 (2001).
96. Parrenin, F. et al. Synchronous change of atmospheric CO_2 and Antarctic temperature during the last deglacial warming. *Science* **339**, 1060–1063 (2013).
97. WAIS Divide Project Members. Precise interpolar phasing of abrupt climate change during the last ice age. *Nature* **520**, 661–665 (2015).
Shows that Greenland temperature changes lead Antarctic temperature changes by ~200 years, suggesting North Atlantic control of D–O variability and an oceanic teleconnection to high southern latitudes.
98. Broecker, W. Paleocean circulation during the last deglaciation: a bipolar seesaw? *Paleoceanography* **13**, 119–121 (1998).
99. Sánchez-Goñi, M., Turon, J.-L., Eynaud, F. & Gendreau, S. European climatic response to millennial-scale changes in the atmosphere–ocean system during the last glacial period. *Quat. Res.* **54**, 394–403 (2000).
100. Sánchez-Goñi, M. et al. Synchroneity between marine and terrestrial responses to millennial scale climatic variability during the last glacial period in the Mediterranean region. *Clim. Dyn.* **19**, 95–105 (2002).
101. Tzedakis, P. et al. Ecological thresholds and patterns of millennial-scale climate variability: the response of vegetation in Greece during the last glacial period. *Geology* **32**, 109–112 (2004).
102. Stockhecke, M. et al. Millennial to orbital-scale variations of drought intensity in the Eastern Mediterranean. *Quat. Sci. Rev.* **133**, 77–95 (2016).
103. Wang, X. et al. Millennial-scale precipitation changes in southern Brazil over the past 90,000 years. *Geophys. Res. Lett.* **34**, L23701 (2007).
104. Kanner, L., Burns, S., Cheng, H. & Edwards, R. L. High-latitude forcing of the South American summer monsoon during the last glacial. *Science* **335**, 570–573 (2013).
105. Mosblech, N. et al. North Atlantic forcing of Amazonian precipitation during the last ice age. *Nat. Geosci.* **5**, 817–820 (2012).
106. Ivanochko, T. et al. Variations in tropical convection as an amplifier of global climate change at the millennial scale. *Earth Planet. Sci. Lett.* **235**, 302–314 (2005).
107. Pausata, F., Battisti, D., Nisancioglu, K. & Bitz, C. Chinese stalagmite $\delta^{18}O$ controlled by changes in the Indian monsoon during a simulated Heinrich event. *Nat. Geosci.* **4**, 474–480 (2011).
108. Marzin, C., Kallel, N., Kageyama, M., Duplessy, J.-C. & Braconnot, P. Glacial fluctuations of the Indian monsoon and their relationship with North Atlantic climate: new data and modelling experiments. *Clim. Past* **9**, 2135–2151 (2013).
109. Lauterbach, S. et al. An ~130 kyr record of surface water temperature and $\delta^{18}O$ from the northern Bay of Bengal: investigating the linkage between Heinrich events and weak monsoon intervals in Asia. *Paleoceanogr. Paleoclimatol.* **35**, e2019PA003646 (2020).
110. Wang, Y. et al. Millennial- and orbital-scale changes in the East Asian monsoon over the past 224,000 years. *Nature* **451**, 1090–1093 (2008).
111. Cheng, H. et al. Ice age terminations. *Science* **326**, 248–252 (2009).
112. Schneider, T., Bischoff, T. & Haug, G. Migrations and dynamics of the intertropical convergence zone. *Nature* **513**, 45–53 (2014).
113. Broecker, W., Peteet, D. & Rind, D. Does the ocean–atmosphere system have more than one stable mode of operation? *Nature* **315**, 21–26 (1985).
One of the first suggestions that the millennial-scale temperature changes observed in Greenland ice cores and in Europe are due to changes in NADW formation and that there could be two quasi-stable modes in the climate system.
114. Menviel, L., Timmermann, A., Mouchet, A. & Timm, O. Climate and marine carbon cycle response to changes in the strength of the southern hemispheric westerlies. *Paleoceanography* **23**, PA4201 (2008).
115. Marcott, S. et al. Ice-shelf collapse from subsurface warming as trigger for Heinrich events. *Proc. Natl Acad. Sci. USA* **108**, 13415–13419 (2011).
Provides evidence for subsurface warming in the North Atlantic during stadials and suggests that this warming led to a destabilization of the LIS.
116. Rainsley, E. et al. Greenland ice mass loss during the Younger Dryas driven by Atlantic meridional overturning circulation feedbacks. *Sci. Rep.* **8**, 11307 (2018).
117. McManus, J. F., Francois, R., Gherardi, J. M., Keigwin, L. D. & Brown-Leger, S. Collapse and rapid resumption of Atlantic meridional circulation linked to deglacial climate changes. *Nature* **428**, 834–837 (2004).
118. Curry, W. B. & Oppo, D. W. Synchronous, high-frequency oscillations in tropical sea surface temperatures and North Atlantic Deep Water production during the last glacial cycle. *Paleoceanography* **12**, 1–14 (1997).
119. Vidal, L. et al. Evidence for changes in the North Atlantic deep water linked to meltwater surges during the Heinrich events. *Earth Planet. Sci. Lett.* **146**, 13–27 (1997).
120. Zahn, R. et al. Thermohaline instability in the North Atlantic during meltwater events: stable isotope and ice-rafted detritus records from core SO75-26KL, Portuguese Margin. *Paleoceanography* **12**, 696–710 (1997).
121. Weldeab, S., Lea, D., Schneider, R. & Andersen, N. 155,000 years of West African Monsoon and ocean thermal evolution. *Science* **316**, 1303–1307 (2007).
122. Hodell, D. et al. An 85-ka record of climate change in lowland Central America. *Quat. Sci. Rev.* **27**, 1152–1165 (2008).
123. Cai, Y. et al. Variability of stalagmite-inferred Indian monsoon precipitation over the past 252,000 y. *Proc. Natl Acad. Sci. USA* **112**, 2954–2959 (2015).
124. Wang, X. et al. Wet periods in northeastern Brazil over the past 210 kyr linked to distant climate anomalies. *Nature* **432**, 740–743 (2004).
125. Leduc, G. et al. Moisture transport across Central America as a positive feedback on abrupt climatic changes. *Nature* **445**, 908–911 (2007).
126. Carolin, S. A. et al. Varied response of western pacific hydrology to climate forcings over the last glacial period. *Science* **340**, 1564–1566 (2013).
127. Timmermann, A. et al. Towards a quantitative understanding of millennial-scale Antarctic warming events. *Quat. Sci. Rev.* **29**, 74–85 (2010).
128. Buiron, D. et al. Regional imprints of millennial variability during the MIS 3 period around Antarctica. *Quat. Sci. Rev.* **48**, 99–112 (2012).
129. Skinner, L., Waelbroeck, C., Scrivner, A. & Fallon, S. Radiocarbon evidence for alternating northern and southern sources of ventilation of the deep Atlantic carbon pool during the last deglaciation. *Proc. Natl Acad. Sci. USA* **111**, 5480–5484 (2014).
130. Gottschalk, J. et al. Biological and physical controls in the Southern Ocean on past millennial-scale atmospheric CO_2 changes. *Nat. Commun.* **7**, 11539 (2016).
131. Jaccard, S., Galbraith, E., Martinez-Garcia, A. & Anderson, R. Covariation of deep Southern Ocean oxygenation and atmospheric CO_2 through the last ice age. *Nature* **530**, 207–210 (2016).
132. Menviel, L., Spence, P. & England, M. Contribution of enhanced Antarctic bottom water formation to Antarctic warm events and millennial-scale atmospheric CO_2 increase. *Earth Planet. Sci. Lett.* **413**, 37–50 (2015).
133. Pedro, J. B. et al. Southern Ocean deep convection as a driver of Antarctic warming events. *Geophys. Res. Lett.* **43**, 2192–2199 (2016).
134. Menviel, L. et al. Southern Hemisphere westerlies as a driver of the early deglacial atmospheric CO_2 rise. *Nat. Commun.* **9**, 2503 (2018).
135. Pedro, J. B. et al. Beyond the bipolar seesaw: toward a process understanding of interhemispheric coupling. *Quat. Sci. Rev.* **192**, 27–46 (2018).

136. Hwang, Y.-T., Frierson, D. M. W. & Kang, S. M. Anthropogenic sulfate aerosol and the southward shift of tropical precipitation in the late 20th century. *Geophys. Res. Lett.* **40**, 2845–2850 (2013).
137. Ceppi, P., Hwang, Y.-T., Liu, X., Frierson, D. & Hartmann, D. The relationship between the ITCZ and the Southern Hemispheric eddy-driven jet. *J. Geophys. Res. Atmos.* **118**, 5136–5146 (2013).
138. Lee, S.-Y., Chiang, J. C. H., Matsumoto, K. & Tokos, K. S. Southern Ocean wind response to North Atlantic cooling and the rise in atmospheric CO_2: modeling perspective and paleoceanographic implications. *Paleoceanography* **26**, PA1214 (2011).
139. Buizert, C. et al. Abrupt ice-age shifts in southern westerly winds and Antarctic climate forced from the north. *Nature* **563**, 681–685 (2018).
140. Toggweiler, J., Russell, J. & Carson, S. Midlatitude westerlies, atmospheric CO_2, and climate change during ice ages. *Paleoceanography* **21**, PA2005 (2006).
141. Ahn, J. & Brook, E. Atmospheric CO_2 and climate on millennial time scales during the last glacial period. *Science* **322**, 83–85 (2008).
142. Stein, K., Timmermann, A., Kwon, E. Y. & Friedrich, T. Timing and magnitude of Southern Ocean sea ice/carbon cycle feedbacks. *Proc. Natl Acad. Sci. USA* **117**, 4498–4504 (2020).
143. Okazaki, Y. et al. Deep water formation in the North Pacific during the last glacial termination. *Science* **329**, 200–204 (2010).
144. Max, L. et al. Pulses of enhanced North Pacific Intermediate Water ventilation from the Okhotsk Sea and Bering Sea during the last deglaciation. *Clim. Past* **10**, 591–605 (2014).
145. Zheng, X. et al. Deepwater circulation variation in the South China Sea since the Last Glacial Maximum. *Geophys. Res. Lett.* **43**, 8590–8599 (2016).
146. Saenko, O., Schmittner, A. & Weaver, A. The Atlantic–Pacific seesaw. *J. Clim.* **17**, 2033–2038 (2004).
147. Chikamoto, M. et al. Variability in North Pacific intermediate and deep water ventilation during Heinrich events in two coupled climate models. *Deep Sea Res. II* **61–64**, 114–126 (2012).
148. Gong, X. et al. Enhanced North Pacific deep-ocean stratification by stronger intermediate water formation during Heinrich Stadial 1. *Nat. Commun.* **10**, 656 (2019).
149. Menviel, L., England, M., Meissner, K., Mouchet, A. & Yu, J. Atlantic-Pacific seesaw and its role in outgassing CO_2 during Heinrich events. *Paleoceanography* **29**, 58–70 (2014).
150. Rasmussen, T., Thomsen, E., Labeyrie, L. & van Weering, T. Circulation changes in the Faeroe-Shetland Channel correlating with cold events during the last glacial period (58–10 ka). *Geology* **24**, 937–940 (1996).
151. Kissel, C., Laj, C., Piotrowski, A., Goldstein, S. & Hemming, S. Millennial-scale propagation of Atlantic deep waters to the glacial Southern Ocean. *Paleoceanography* **23**, PA2102 (2008).
152. Fleitmann, D. et al. Timing and climatic impact of Greenland interstadials recorded in stalagmites from northern Turkey. *Geophys. Res. Lett.* **36**, L19707 (2009).
153. Fletcher, W. et al. Millennial-scale variability during the last glacial in vegetation records from Europe. *Quat. Sci. Rev.* **29**, 2839–2864 (2010).
154. Müller, U. et al. The role of climate in the spread of modern humans into Europe. *Quat. Sci. Rev.* **30**, 273–279 (2011).
155. Brook, E. J., Harder, S., Severinghaus, J., Steig, E. & Sucher, C. On the origin and timing of rapid changes in atmospheric methane during the last glacial period. *Glob. Biogeochem. Cycles* **14**, 559–572 (2000).
156. Chappellaz, J. et al. Synchronous changes in atmospheric CH_4 and Greenland climate between 40 and 8 kyr BP. *Nature* **366**, 443–445 (1993).
157. Brook, E. J., Sowers, T. & Orchardo, J. Rapid variations in atmospheric methane concentrations during the past 110,000 years. *Science* **273**, 1087–1091 (1996).
158. Bergamaschi, P. et al. Satellite chartography of atmospheric methane from SCIAMACHY on board ENVISAT: 2. Evaluation based on inverse model simulations. *J. Geophys. Res. Atmos.* **112**, D02304 (2007).
159. Rhodes, R. et al. Enhanced tropical methane production in response to iceberg discharge in the North Atlantic. *Science* **348**, 1016–1019 (2015).
160. Tzedakis, P., Pälike, H., Roucoux, K. & de Abreu, L. Atmospheric methane, southern European vegetation and low-mid latitude links on orbital and millennial timescales. *Earth Planet. Sci. Lett.* **277**, 307–317 (2009).
161. Timmermann, A., Schulz, M., Gildor, H. & Tziperman, E. Coherent resonant millennial-scale climate oscillations triggered by massive meltwater pulses. *J. Clim.* **16**, 2569–2585 (2003).
162. Alley, R. B., Anandakrishnan, S. & Jung, P. Stochastic resonance in the North Atlantic. *Paleoceanography* **16**, 190–198 (2001).
163. Ganopolski, A. & Rahmstorf, S. Abrupt glacial climate changes due to stochastic resonance. *Phys. Rev. Lett.* **88**, 038501 (2002).
164. Krebs, U. & Timmermann, A. Tropical air–sea interactions accelerate the recovery of the Atlantic meridional overturning circulation after a major shutdown. *J. Clim.* **20**, 4940–4956 (2007).
165. Richter, I. & Xie, S.-P. Moisture transport from the Atlantic to the Pacific basin and its response to North Atlantic cooling and global warming. *Clim. Dyn.* **35**, 551–566 (2010).
166. Friedrich, T. et al. The mechanism behind internally generated centennial-to-millennial scale climate variability in an earth system model of intermediate complexity. *Geosci. Model Dev.* **3**, 377–389 (2010).
167. Drijfhout, S., Gleeson, E., Dijkstra, H. A. & Livina, V. Spontaneous abrupt climate change due to an atmospheric blocking–sea-ice–ocean feedback in an unforced climate model simulation. *Proc. Natl Acad. Sci. USA* **110**, 19713–19718 (2013).
168. Kleppin, H., Jochum, M., Otto-Bliesner, B., Shields, C. A. & Yeager, S. Stochastic atmospheric forcing as a cause of Greenland climate transitions. *J. Clim.* **28**, 7741–7763 (2015).
169. Singh, H. A., Battisti, D. S. & Bitz, C. M. A heuristic model of Dansgaard–Oeschger cycles. Part I: description, results, and sensitivity studies. *J. Clim.* **27**, 4337–4358 (2014).
170. Petersen, S., Schrag, D. & Clark, P. A new mechanism for Dansgaard-Oeschger cycles. *Paleoceanography* **28**, 24–30 (2013).
171. Boers, N., Ghil, M. & Rousseau, D.-D. Ocean circulation, ice shelf, and sea ice interactions explain Dansgaard–Oeschger cycles. *Proc. Natl Acad. Sci. USA* **115**, E11005–E11014 (2018).
172. Hulbe, C. L., MacAyeal, D. R., Denton, G. H., Kleman, J. & Lowell, T. V. Catastrophic ice shelf breakup as the source of Heinrich event icebergs. *Paleoceanography* **19**, PA1004 (2004).
173. Cofaigh, C. et al. The role of meltwater in high-latitude trough-mouth fan development: the Disko Trough-Mouth Fan, West Greenland. *Mar. Geol.* **402**, 17–32 (2018).
174. Jennings, A. E. et al. Baffin Bay paleoenvironments in the LGM and HS1: resolving the ice-shelf question. *Mar. Geol.* **402**, 5–16 (2018).
175. Obase, T. & Abe-Ouchi, A. Abrupt Bølling-Allerød warming simulated under gradual forcing of the last deglaciation. *Geophys. Res. Lett.* **46**, 11397–11405 (2019).
176. Guo, C., Nisancioglu, K. H., Bentsen, M., Bethke, I. & Zhang, Z. Equilibrium simulations of Marine Isotope Stage 3 climate. *Clim. Past* **15**, 1133–1151 (2019).
177. Marshall, S. & Koutnik, M. Ice sheet action versus reaction: distinguishing between Heinrich events and Dansgaard-Oeschger cycles in the North Atlantic. *Paleoceanography* **21**, PA2021 (2006).
178. Alvarez-Solas, J., Banderas, R., Robinson, A. & Montoya, M. Ocean-driven millennial-scale variability of the Eurasian ice sheet during the last glacial period simulated with a hybrid ice-sheet–shelf model. *Clim. Past* **15**, 957–979 (2019).
179. Zhang, X., Prange, M., Merkel, U. & Schulz, M. Instability of the Atlantic overturning circulation during Marine Isotope Stage 3. *Geophys. Res. Lett.* **41**, 4285–4293 (2014).
180. Yokoyama, Y., Esat, T. & Lambeck, K. Coupled climate and sea-level changes deduced from Huon Peninsula coral terraces of the last ice age. *Earth Planet. Sci. Lett.* **193**, 579–587 (2001).
181. Chappell, J. Sea level changes forced ice breakouts in the last glacial cycle: new results from coral terraces. *Quat. Sci. Rev.* **21**, 1229–1240 (2002).
182. Rohling, E., Marsh, R., Wells, N., Siddall, M. & Edwards, N. Similar meltwater contributions to glacial sea level changes from Antarctic and northern ice sheets. *Nature* **430**, 1016–1021 (2004).
183. Arz, H. W., Lamy, F., Ganopolski, A., Nowaczyk, N. & Pätzold, J. Dominant Northern Hemisphere climate control over millennial-scale glacial sea-level variability. *Quat. Sci. Rev.* **26**, 312–321 (2007).
184. MacAyeal, D. Binge/purge oscillations of the Laurentide ice sheet as a cause of the North Atlantic's Heinrich events. *Paleoceanography* **8**, 775–784 (1993).
Suggests that Heinrich events are due to growth–purge oscillations of the LIS.
185. Calov, R., Ganopolski, A., Petoukhov, V., Claussen, M. & Greve, R. Large-scale instabilities of the Laurentide ice sheet simulated in a fully coupled climate-system model. *Geophys. Res. Lett.* **29**, 2216 (2002).
186. Calov, R. et al. Results from the Ice-Sheet Model Intercomparison Project–Heinrich Event INtercOmparison (ISMIP HEINO). *J. Glaciol.* **56**, 371–383 (2010).
187. Shaffer, G., Olsen, S. & Bjerrum, C. Ocean subsurface warming as a mechanism for coupling Dansgaard-Oeschger climate cycles and ice-rafting events. *Geophys. Res. Lett.* **31**, L24202 (2004).
188. Mignot, J., Ganopolski, A. & Levermann, A. Atlantic subsurface temperatures: response to a shutdown of the overturning circulation and consequences for its recovery. *J. Clim.* **20**, 4884–4898 (2007).
189. Massom, R. et al. Antarctic ice shelf disintegration triggered by sea ice loss and ocean swell. *Nature* **558**, 383–389 (2018).
190. Greene, C. A., Young, D. A., Gwyther, D. E., Galton-Fenzi, B. K. & Blankenship, D. D. Seasonal dynamics of Totten Ice Shelf controlled by sea ice buttressing. *Cryosphere* **12**, 2869–2882 (2018).
191. Alvarez-Solas, J. et al. Links between ocean temperature and iceberg discharge during Heinrich events. *Nat. Geosci.* **3**, 122–126 (2010).
192. Alvarez-Solas, J., Robinson, A., Montoya, M. & Ritz, C. Iceberg discharges of the last glacial period driven by oceanic circulation changes. *Proc. Natl Acad. Sci. USA* **110**, 16350–16354 (2013).
193. Tabone, I., Robinson, A., Alvarez-Solas, J. & Montoya, M. Impact of millennial-scale oceanic variability on the Greenland ice-sheet evolution throughout the last glacial period. *Clim. Past* **15**, 593–609 (2019).
194. Bassis, J., Petersen, S. & Cathles, L. M. Heinrich events triggered by ocean forcing and modulated by isostatic adjustment. *Nature* **542**, 332–334 (2017).
195. Roberts, W. H. G., Valdes, P. J. & Payne, A. J. Topography's crucial role in Heinrich Events. *Proc. Natl Acad. Sci. USA* **111**, 16688–16693 (2014).
196. Andres, H. J. & Tarasov, L. Towards understanding potential atmospheric contributions to abrupt climate changes: characterizing changes to the North Atlantic eddy-driven jet over the last deglaciation. *Clim. Past* **15**, 1621–1646 (2019).
197. Ziemen, F. A., Kapsch, M.-L., Klockmann, M. & Mikolajewicz, U. Heinrich events show two-stage climate response in transient glacial simulations. *Clim. Past* **15**, 153–168 (2019).
198. Carlson, A. E., Tarasov, L. & Pico, T. Rapid Laurentide ice-sheet advance towards southern last glacial maximum limit during marine isotope stage 3. *Quat. Sci. Rev.* **196**, 118–123 (2018).
199. Clark, P. U. et al. Freshwater forcing of abrupt climate change during the last glaciation. *Science* **293**, 283–287 (2001).
200. Galaasen, E. V. et al. Rapid reductions in North Atlantic Deep Water during the peak of the last interglacial period. *Science* **343**, 1129–1132 (2014).
201. Tzedakis, P. et al. Enhanced climate instability in the North Atlantic and southern Europe during the Last Interglacial. *Nat. Commun.* **9**, 4235 (2018).
202. Galaasen, E. V. et al. Interglacial instability of North Atlantic Deep Water ventilation. *Science* **367**, 1485–1489 (2020).
203. Irvali, N. et al. Evidence for regional cooling, frontal advances, and East Greenland Ice Sheet changes during the demise of the last interglacial. *Quat. Sci. Rev.* **150**, 184–199 (2016).
204. Oka, A., Hasumi, H. & Abe-Ouchi, A. The thermal threshold of the Atlantic meridional overturning circulation and its control by wind stress forcing during glacial climate. *Geophys. Res. Lett.* **39**, L09709 (2012).
205. Hu, A. et al. Role of the Bering Strait on the hysteresis of the ocean conveyor belt circulation and glacial climate stability. *Proc. Natl Acad. Sci. USA* **107**, 6417–6422 (2012).
206. Hu, A. et al. Effects of the Bering Strait closure on AMOC and global climate under different background climates. *Prog. Oceanogr.* **132**, 174–196 (2015).
207. de Boer, A. M. & Nof, D. The exhaust valve of the North Atlantic. *J. Clim.* **17**, 417–422 (2004).
208. Menviel, L. et al. Removing the North Pacific halocline: effects on global climate, ocean circulation and the

carbon cycle. *Deep Sea Res. II* **61–64**, 106–113 (2012).
209. Curry, W. & Oppo, D. Glacial water mass geometry and the distribution of $\delta^{13}C$ of ΣCO_2 in the western Atlantic Ocean. *Paleoceanography* **20**, PA1017 (2005).
210. Marchitto, T. & Broecker, W. Deep water mass geometry in the glacial Atlantic Ocean: a review of constraints from the paleonutrient proxy Cd/Ca. *Geochem. Geophys. Geosyst.* **7**, Q12003 (2006).
211. Lynch-Stieglitz, J. et al. Meridional overturning circulation in the South Atlantic at the last glacial maximum. *Geochem. Geophys. Geosyst.* **7**, Q10N03 (2006).
212. Menviel, L. et al. Poorly ventilated deep ocean at the Last Glacial Maximum inferred from carbon isotopes: a data-model comparison study. *Paleoceanography* **32**, 2–17 (2017).
213. Skinner, L. et al. Radiocarbon constraints on the glacial ocean circulation and its impact on atmospheric CO_2. *Nat. Commun.* **8**, 16010 (2017).
214. Muglia, J. & Schmittner, A. Glacial Atlantic overturning increased by wind stress in climate models. *Geophys. Res. Lett.* **42**, 9862–9868 (2015).
215. Kageyama, M. et al. The PMIP4-CMIP6 Last Glacial Maximum experiments: preliminary results and comparison with the PMIP3-CMIP5 simulations. *Clim. Past Discuss.* **2020**, 1–37 (2020).
216. Sherriff-Tadano, S., Abe-Ouchi, A., Yoshimori, M., Oka, A. & Chan, W.-L. Influence of glacial ice sheets on the Atlantic meridional overturning circulation through surface wind change. *Clim. Dyn.* **50**, 2881–2903 (2018).
217. Born, A. & Stocker, T. F. Two stable equilibria of the Atlantic subpolar gyre. *J. Phys. Oceanogr.* **44**, 246–264 (2014).
218. Li, C. & Born, A. Coupled atmosphere-ice-ocean dynamics in Dansgaard-Oeschger events. *Quat. Sci. Rev.* **203**, 1–20 (2019).
219. Heuzé, C. North Atlantic deep water formation and AMOC in CMIP5 models. *Ocean Sci.* **13**, 609–622 (2017).
220. Jensen, M. F., Nisancioglu, K. H. & Spall, M. A. Large changes in sea ice triggered by small changes in Atlantic water temperature. *J. Clim.* **31**, 4847–4863 (2018).
221. Menviel, L. C. et al. Enhanced mid-depth southward transport in the northeast Atlantic at the last glacial maximum despite a weaker AMOC. *Paleoceanogr. Paleoclimatol.* **35**, e2019PA003793 (2020).
222. Toggweiler, J. & Samuels, B. Effect of Drake Passage on the global thermohaline circulation. *Deep Sea Res. I* **42**, 477–500 (1995).
223. Delworth, T. L. & Zeng, F. Simulated impact of altered Southern Hemisphere winds on the Atlantic meridional overturning circulation. *Geophys. Res. Lett.* **35**, L20708 (2008).
224. Gent, P. R. Effects of Southern Hemisphere wind changes on the meridional overturning circulation in ocean models. *Annu. Rev. Mar. Sci.* **8**, 79–94 (2016).
225. Swingedouw, D., Fichefet, T., Goosse, H. & Loutre, M.-F. Impact of transient freshwater releases in the Southern Ocean on the AMOC and climate. *Clim. Dyn.* **33**, 365–381 (2009).
226. Martin, T., Park, W. & Latif, M. Multi-centennial variability controlled by Southern Ocean convection in the Kiel Climate Model. *Clim. Dyn.* **40**, 2005–2022 (2013).
227. Bond, G. et al. A pervasive millennial-scale cycle in North Atlantic Holocene and glacial climates. *Science* **278**, 1257–1266 (1997).
228. Schulz, M., Paul, A. & Timmermann, A. Relaxation oscillators in concert: a framework for climate change at millennial timescales during the late Pleistocene. *Geophys. Res. Lett.* **29**, 2193 (2002).
229. Svensson, A. et al. A 60,000 year Greenland stratigraphic ice core chronology. *Clim. Past* **4**, 47–57 (2008).
230. Bereiter, B. et al. Mode of change of millennial CO_2 variability during the last glacial cycle associated with a bipolar marine carbon seesaw. *Proc. Natl Acad. Sci. USA* **109**, 9755–9760 (2012).
231. Locarnini, R. et al. *World Ocean Atlas 2013* Vol. 1, 40 pp (NOAA Atlas NESDIS 73, 2013).
232. Bullister, J. L., Rhein, M. & Mauritzen, C. in *Ocean Circulation and Climate* Vol. 103 Ch. 10 (eds Siedler, G., Griffies, S. M., Gould, J. & Church, J. A.) 227–253 (Academic, 2013).
233. Cunningham, S. A. et al. Temporal variability of the Atlantic meridional overturning circulation at 26.5°N. *Science* **317**, 935–938 (2007).
234. Ferrari, R. & Ferreira, D. What processes drive the ocean heat transport? *Ocean Model.* **38**, 171–186 (2011).

Acknowledgements
L.C.M. acknowledges funding from the Australian Research Council (grant nos. FT180100606 and DP180100048). P.C.T acknowledges funding from the UK Natural Environment Research Council (grant no. NE/R000204/1).

Author contributions
L.C.M. wrote the manuscript, with contributions from L.C.S., L.T. and P.C.T. All authors contributed to the ideas in this paper.

Competing interests
The authors declare no competing interests.

Peer review information
Nature Reviews Earth & Environment thanks J. Lynch-Stieglitz, J. Rheinlænder, X. Zhang and the other anonymous reviewer(s) for their contribution to the peer review of this work.

Supplementary information
Supplementary information is available for this paper at https://doi.org/10.1038/s43017-020-00106-y.